=

INFLUENCE OF PROCESS PARAMETERS ON BIOACTIVITY OF CaF_2-MgF_2 CONTAINING BOROSILICATE GLASS CERAMICS

Thesis submitted in partial fulfilment of the requirement for the award of the degree of

Masters of Physics

Submitted by

Anandita Arora

(301504005)

Under the guidance of

Dr. Kulvir Singh

(Professor**)**

School of Physics and Materials Science

Thapar University, Patiala-147004

Punjab

July, 2017

To my wonderful family, an inspiration in

everything i do...

Thank You...

CERTIFICATE

I hereby declare that the report entitled "**INFLUENCE OF PROCESS PARAMETERS ON BIOACTIVITY OF CaF_2-MgF_2 CONTAINING BOROSILICATE GLASS CERAMICS** " is an authentic record of my own work carried out for the partial fulfilment of the requirement for the award of degree of M.Sc. (Masters of Science) at Thapar University, Patiala (Punjab), under the guidance of **Dr. Kulvir Singh** (School of Physics and Materials Science). The matter presented in the dissertation has not been submitted in part or full for the award of any degree.

Anandita

Anandita Arora

Date: July, 2017

Roll No.: 301504005

It is certified that the above statement made by the candidate is correct to the best of my knowledge and belief.

18/7/17

Dr. Kulvir Singh

Professor

School of Physics and Materials Science

Thapar University, Patiala

Acknowledgement

I would like to take this opportunity to express my gratitude and appreciation to everyone that helped me in some way whilst completing this research. Special recognition and thanks goes to my supervisor professor **Dr. Kulvir Singh** for providing inspiring motivation, different solutions, and kind guidance towards my master thesis. He has provided me with his valuable time in discussing, going through my draft, providing comments and advising me on how to improve my work from time to time.

I would like to give many thanks to **Dr. Manoj Sharma**, Prof. and Head, **Dr O.P Pandey**, **Dr. Bhaskar Chandra Mohanty, Dr. Puneet Sharma, Dr. B. N. Chudasama** for allowing me to use the facilities in Materials Research Lab and the opportunity to work on this project.

I would like to give my special thanks to **Dr. Satwinder Singh Danewalia,** Research Scholar **Ms. Neetu Bansal** for guiding me throughout this journey with the experimental work and cooperating with me constantly.

I would also like to thank some professional people from the institution for their suggestion, comments, information, material and other help. They are **Dr. Gurbinder Kaur, Mr. Ayush Gupta, Mr. Savidh Khan, Mr. Gaurav Sharma, Ms. Indu Gupta, Ms Shivani Jindal, Ms. Paramvir Kaur, Ms. Trisha and Ms. Shivani.**

I am also thankful to SAI Labs, Thapar University, CIL Lab, Panjab University and **Dr. Sachin Tyagi, Ms. Pooja Sharma, Ms Sarita and Mr. Virender, CSIR-CSIO,** Chandigarh for allowing me to use their facilities in characterisation and research work.

Contents

List of figures

List of tables

Abstract

Calcium and magnesium fluoride containing borosilicate glass ceramics with the composition $52SiO_2$-$18B_2O_3$-(30-*x*) MgF_2-*x* CaF_2 (*x* = 5,30) are synthesized by sol-gel chemical route. During synthesis, the process parameters are changed along with change in solvent. Samples are prepared using inorganic compounds (calcium carbonate, magnesium oxide, boric acid, tetra ethyl ortho silicate (TEOS) and hydrofluoric acid) in de-ionized water. The as prepared samples are studied by various techniques to study the effect of process parameters on structural correlated properties. The XRD patterns of the samples exhibit different crystalline phases. The crystallinity index of these phases changes with process parameters. The bioactivities of these as prepared samples are checked by *in-vitro* method. The heat treated samples show some bioactive properties.

Chapter 1. Introduction

Due to the increase in number of bone and trauma diseases in the last decade, there is need for artificial grafts that can successfully replicate human bone and tissues. Tissue engineering has emerged as a promising field for the repair and regeneration of tissues and organs lost or damaged as a result of injuries or age related diseases [1,2]. When hydroxyapatite was believed to be the best biocompatible replacement material, Hench in 1969, developed a material called bioglass, containing calcium and phosphorous which bonds to broken bones. This material mimics living bone materials to a large extent and stimulates the regrowth of new bones and tissues. Due to its biocompatibility and osteogenic properties, it came to be known as "bioactive glass or bioglass". Bioactive glasses, especially silicate and borate based materials, are known to play a fundamental role in this field due to their osteoconductive, osteoproductive and osteoinductive properties. In the field of biomaterial sciences, bioglass along with synthetic hydroxyapatite (HAP) are known as "bioactive ceramics". These bioactive materials have the potential to fulfil the need of living tissues and organs required for transplantation. In a general sense, a bioactive material may be defined as a material that is designed to induce a specific biological activity [3]. It undergoes specific surface reactions with the body surroundings, leading to the formation of a bone like layer- hydroxyapatite (HAP), which are responsible for the formation of a firm bond with hard and soft tissues [4]. The ability of materials to form an HAP-like surface layer when immersed in a simulated body fluid (SBF) is often taken as an indication of its bioactivity [5]. This external test to check the bioactivity of the developed materials is called *in-vitro* test.

1.1 Classification of bio-materials

In general, biomaterials can be categorized based on the interaction with tissue. The behaviour of the implanted biomaterial in body fluids may vary with its composition [6]. It can be categorized as follows:

1.1.1 Bio-inert

The materials/scaffolds which do not show any interaction with the host tissues are known as bio-inert implants. In this case a capsule of tissues surrounds the implanted materials. These materials find applications in dentistry where high chemical durability, resistance to pH change is required, e.g: alumina, zirconia.

1.1.2 Bio-resorbable

The materials like tri-calcium phosphate, calcium phosphate, hydroxyapatite helps the growth of tissues on their surface. They are generally used to treat fractured bones and they also act as filler for cracks in the bones, e.g: tricalcium phosphate.

1.1.3 Bioactive

When a material is able to form a bond (HAP layer on its surface) with the host tissue that is called a "bioactive" materials. The bond forming kinetics is highly dependent on materials composition, e.g: bioactive glasses, glass-ceramics.

1.2 Requirements of bioactive materials [6]

i. **Ability to deliver cells:** The material should be non-toxic and biocompatible, stimulating cell attachment, differentiation, and proliferation.

ii. **Osteoconductivity:** The material should encourage osteoconduction with the host bone. Osteoconductivity brings about a strong bond between the scaffold and host bone.

iii. **Biodegradability:** The scaffold should lead to biodegradation *in vivo* at rates appropriate to tissue regeneration.

iv. **Mechanical properties:** The mechanical strength of the scaffold is determined by both the properties of the biomaterial and the porous structure. It should be sufficient to provide mechanical stability at load bearing sites prior to synthesis of new extracellular matrix by cells.

v. **Porous structure:** The scaffold should have an interconnected porous structure with porosity >90% and diameters between (300-500) μm for cell penetration, tissue in growth, vascularisation, and nutrient delivery.

vi. **Fabrication:** The material should possess desired fabrication capability, e.g., being readily produced into irregular shapes of scaffolds that match the defects in bone of individual patients.

vii. Hench and Polak [7] termed the bioactive and biodegradable materials as third generation biomaterials. Bioinert materials, as the first and second generation comprises of interactive materials such as bioactive ceramics and biodegradable polymers. In search for this new generation of materials, bioglass compositions are being optimised at various scales.

1.3 Effect of constituents of glasses on bioactivity

The properties of a material depends on atomic arrangement, chemical nature, structure and composition. Different components have different contribution to the overall behaviour and bioactivity of the glasses. The role of fluoride is very important in prevention of caries as it forms fluorapatite (FAP) by replacing hydroxyl ions in the apatite structure. FAP formed is more acid resistant than hydroxyl carbonated apatite (HCA) and is the main component of the enamel and the dentine [8]. The advantage of bioactive glasses to form apatite layer in body fluids is used in toothpastes for treating dentine hypersensitivity [9]. When dentinal tubules of root dentine are exposed specially to hot and cold food it results in dentine hypersensitivity. The toothpaste contains bioactive glass. Its particles are small enough to enter the dentinal tubules. The formation of apatite thereby stops the direct contact of the roots with any food or fluid, thus reducing hyper sensitivity. Formation of FAP is appreciated, rather than HCA, as it is chemically more stable and does not dissolve when mouth is exposed to acidic conditions [8]. Dental care with bioglass is not limited to toothpaste only. Bleaching treatment of teeth, for which hydrogen peroxide was used earlier is now replaced by a better alternative. Dentists

often use air polishing to brighten the teeth, which is a technique that uses ceramic (traditionally sodium bicarbonate) as abrasives to remove stains. The results of incorporation of fluorine in bioactive glasses generates immense interest in its biomedical applications [10]. The significant increase in the quantity of bone tissue formed around the boron-bioglass particles indicates osteoconductive effects of boron doped bioactive glasses [11]. More *in vitro* studies on boron modified bioactive glasses are needed to clearly identify the effect of these glasses on human cells and to confirm the potential simulating effects of boron [12].

Magnesium (Mg) stimulates new bone formation. It is a minor constituent required for bone, teeth and adenosine triphosphate (ATP). It also increases bone cell adhesion and stability which is probably due to interactions with integrins [13]. Mg is suggested to interact with integrins of osteoblast cells which are responsible for cell adhesion and stability. It has been observed that Mg depletion results in impaired bone growth, increased bone resorption and loss in trabecular bone underlining the significant role that Magnesium plays in bone metabolism [13,14]. Silica is known to be an excellent and essential element for metabolic processes associated with the formation and calcification of bone tissues. High silica contents have been detected in early stages of bone matrix calcification. Alongside this, aqueous silica has the property to induce precipitation of hydroxyapatite which is the inorganic phase of human bone [15]. Fluoride prevents demineralization and increases remineralization. For the prevention of caries, the role of fluoride is very important as it forms FAP by replacing hydroxyl ions in apatite structure. This substitution has a profound effect on chemical stability of the apatite formed *in vivo.* Calcium is the main component of biological apatite, the inorganic phase of human bone and plays an essential role in bone formation and resorption. It is present in bones and teeth and helps in the regulation of nerves, enzyme activation and neuromuscular excitability. Calcium increases the expression of insulin like growth factors, which regulate human osteoblast formation [6,16].

1.4 Glasses as a bioactive materials

A major hurdle that comes in the designing of the bioactive scaffolds is that most materials are not mechanically competent and bio-resorbable at the same time. In a broader sense, mechanically strong materials are usually not bioactive, while degradable materials tend to be mechanically weaker [17]. Bioactive glasses are a subset of inorganic bioactive materials, which are capable of reacting with physiological fluids to form tenacious bonds to bone [18]. The excellent properties of bioactive glasses and their long history of applications in biomedical implants [18] has prompted to extensive research in the last 10 years. Although bioactive glasses are mechanically weak, it has been seen that 45S5 (bioglass) can partially crystallise when heated to high temperatures (>950°C) during scaffold fabrication. Such mechanically strong crystalline phase can transform to a biodegradable, amorphous calcium phosphate phase in a biological environment [19,20]. This step enables the two normally irreconcilable properties, i.e. mechanical competence and biodegradability, to be combined in a single scaffold.

1.5 Types of glasses

Figure 1.1 indicates the components of glass and their respective roles in the formation of glasses. Generic name of the glass is usually derived from its network former. It is important to get a deep understanding into the glass and its structural design. Bioactive glasses can be categorized on the basis of the network former present in them as follows:

1.5.1 Silicate glasses: In general, silica has been the main component as an oxide in the glass matrix. Each Oxygen anion is coordinated by two silica cations, corresponding to corner sharing of the oxide tetrahedral, preventing the close-packing of anion layers and resulting in relatively open structures [21]. Silicate bioactive glasses (45S5 or 13-93) are well known to assist the enhancement function of osteoblastic cells such as murine MC3T3-E1 cells, during the conventional *in vitro* cell culture [22].

1.5.2 Borate/ Borosilicate glasses: The 45S5 silicate glass composition has been studied widely up till now but borosilicate glass compositions have been recently explored. Boron is a trace element required for healthy bones [11]. And so, it was introduced to silicate bioactive glasses to improve the bioactivity and structure of the material for medical applications.

1.5.3 Oxyfluoride glasses: Oxyfluoride glasses are of immense interest as they contain considerable amount of rare earth elements. New optical effects can be observed due to presence of high amount of rare earth ions in the glass. Glass structure and connectivity are effected when fluorine gets exchanged by oxygen. They are suitable for use in lasers [23].

1.5.4 Fluoride glasses: Incorporation of fluorine in the bioactive glasses decreases its T_g, which leads to less crystalline and more bioactive glass. Fluoride is well known to promote remineralization [24].

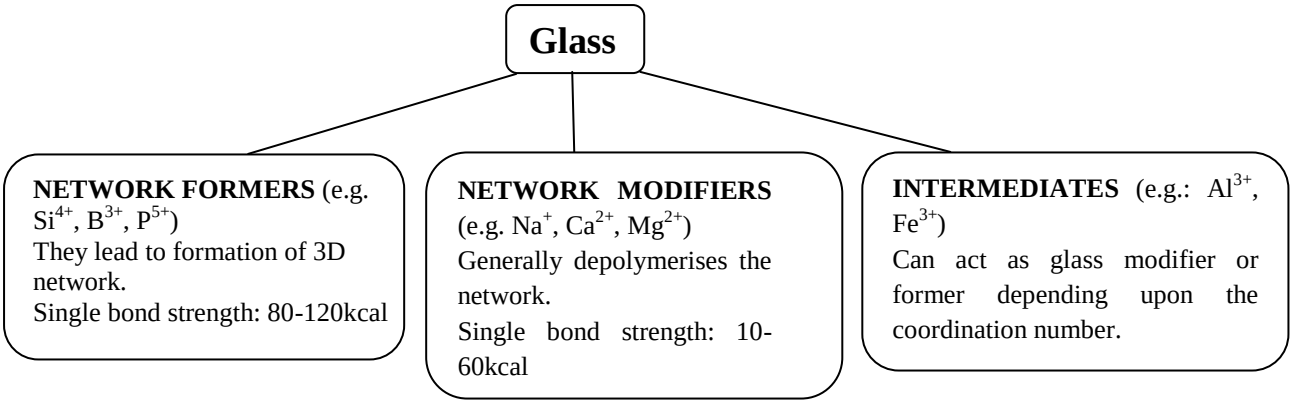

Figure 1.1 Glass and various components.

The properties of glasses are easily tailored to choose proper modifier/intermediate oxides like MgO, K_2O, Na_2O, LiO_2, Al_2O_3, Cr_2O_3 and TiO_2 etc.

1.6 Method of preparation:

Most of the traditional glasses are inorganic and non-metallic, but currently large numbers of organic glasses are in front line and they need different preparation techniques. Most commonly used methods are described below:

1.6.1 Melt-quenching: Melt-quenching is the oldest method being used for the preparation of glass. In this technique the material is heated to high temperature, near melting point and then rapidly cooled to form glass. Rates of cooling required for glassy phase formation are different for different materials. For example certain glass formers such as B_2O_3, P_2O_5 etc. will form glassy phase even under conditions of slow cooling (like 1K/s). The main drawback of using this method is the high temperature required which makes it less energy efficient. Also, there is a high probability of contamination in sample due to use of alumina crucible. Many glass compositions, involving fluorine are difficult to synthesize using this route.

1.6.2 Sol-Gel method: Sol-gel process is defined as the chemical synthesis of inorganic materials by preparation of a sol, gelation of the sol (gel) and removal of the solvent. The sol-gel process involves the transition of a system from a liquid "sol" into a solid "gel" phase. The chemistry involved in the process is based on inorganic polymerisation reactions of metal alkoxides. It allows for the generation of a “pre” cross linking network in solution with high purity. Low processing temperature helps in energy saving and also minimises contamination. Gel is an elastic solid matter produced abruptly from a viscous liquid by a process involving continuous polymerization. Gel, which is amorphous and homogeneous, is heated to remove volatile components and produce an initial densification, followed by a final process of calcination at appropriate temperature. Advantage of sol-gel technique is that many materials can be prepared homogeneously at a relatively lower temperature, especially below the melting point. In addition, the purity of the materials can be improved as the starting materials can be purified to the desired extent by various techniques. Even though the process appears to be simple, the reactions are very sensitive to the external conditions like temperature, concentration of solutions, reaction time etc. The main disadvantage of this process is to get proper organometallic precursors for cations. Sol-gel processing is an ideal method to attain compositional and structural control [25].

1.7 Details of sol-gel process

The applications of sol-gel materials are diverse, covering optics, electronics, chemistry and biology. The foundation for sol-gel fabrication was laid in the late 1800s by Ebelman and Graham. Initiating the process from soluble molecular precursors, the reaction follows an inorganic polymerization. The process involves hydrolysis, polymerization, gelation, drying, and a dehydration process. The reaction takes place generally at room temperature, the solvent being either water or organic. There is a wide pH range and conditions under which this process can materialize. The conversion from a liquid state (clear or colloidal solution) to a solid (di or multiphase gel) explains the name of the "sol-gel process". The preparation of new materials by the sol-gel method consists of the following steps:

Step 1. ***Mixing:*** Favourable choices for use in the preparation of silica-based gels are tetramethoxysilane, $Si(OCH_3)_4$, and tetraethoxysilane, $Si(OC_2H_5)_4$, known as TMOS and TEOS, respectively. The liquid silicon alkoxide precursor $Si(OR)_4$ reacts with water and undergoes hydrolysis and polycondensation reactions, in the presence of a common solvent. Silicate/Borosilicate gels are synthesized by utilizing an acid (e.g.HCl/HNO_3) or a base (e.g. NH_3) as a catalyst. Two hydrolyzed Si-OH molecules are linked together in the condensation reaction to form a siloxane (Si-O-Si) bond. The presence of excess water along with the catalyst helps the reaction move forward.

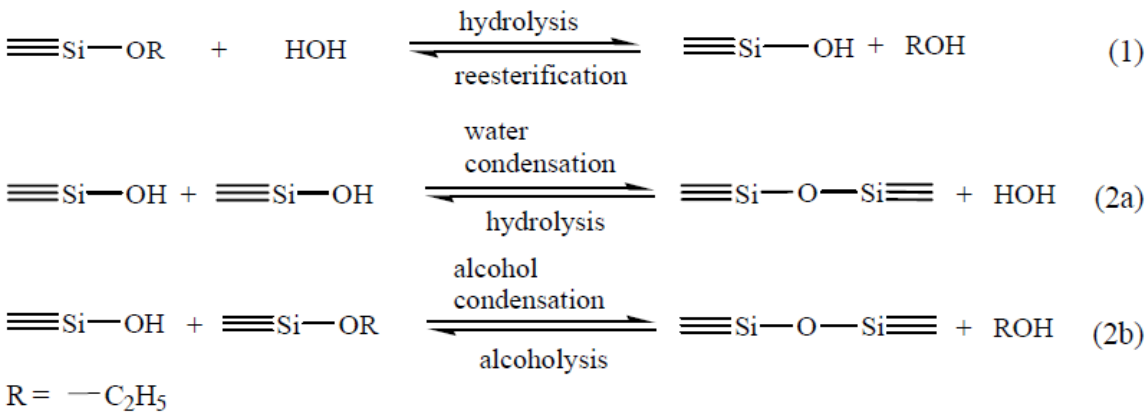

Figure 1.2 Schematic of reactions in the mixing step of the sol–gel process [25].

Step 2. ***Casting and gelation***: Being low in viscosity, the sol can be cast into a mould which does not leads to adhesion of the gel. During gelation, the colloidal particles in the solution link together to form a three dimensional network. Thus the gel is a substance that contains a continuous solid skeleton enclosing a continuous liquid phase. Gels can be defined as strong or weak depending on whether the bond connecting the solid phase is permanent or reversible. The difference between strong and weak is a matter of time scale. Its morphology can range from being discrete to continuous polymer network [6]. The gel is wet due to the water from the solution and ethanol produced during the condensation reactions.

Step 3. ***Aging of gel:*** Also known as *syneresis*, this step requires the gel to be kept at certain temperature (usually room temperature) for a couple of hours to days. In the course of this time polycondensation and reprecipitation of the gel network takes place which decreases the porosity and increases the strength of the network. Properly aged gel must mature with enough strength to avoid cracking during drying.

Step 4. ***Drying:*** This step involves removal of condensation by-products, such as water and alcohol leaving behind interstitial nanopores. The polymer chain aggregation increases as the gel is dried at room temperature. The ousting of surface silanol (Si-OH) bonds from the pore network leads to a chemically stable ultra porous solid.

Step 5. ***Stabilizing:*** For the purpose of elimination of pores, densification to occur, removal of nitrates and stabilizing of the as formed product it is thus dried at high temperatures ranging from 400°C-800°C. Material is converted into clear massive glass by sintering process.

1.8 Effect of the process parameters

The nature of reagents used, the molar ratio between the precursors, the type of solvent, synthesis temperature, pH, etc are the factors that immensely influence the network formation within the microstructure and the properties of the resulting material. The particle size of the

solution and the cross-linking within the particles (i.e. the density) depend upon the pH and *R'* ratio *(R'* = $[H_2O]/[Si(OR)]$) among other variables . Also, the fabrication method plays a pivotal role in determining the structural properties of the biomaterial [26].

1.8.1 The precursors

Alkoxides are the most commonly used sol-gel precursors. Good homogeneity in the reaction between alkoxysilanes and water makes SiO_2 formation the most investigated in the sol-gel literature.

The most used alkoxysilane precursors for sol-gel technique are [27]:

i. Tetra ethyl orthosilicate (TEOS),
ii. Tetra methyl orthosilicate (TMOS),
iii. Methyl tri-ethoxysilane (MTES),
iv. Methyl tri-methoxysilane (MTMS),
v. Vinyl tri-methoxysilane (VTMS),
vi. 3-aminopropyl tri-methoxysilane (APS).

TEOS is often used as a precursor for the synthesis of SiO_2, as it reacts readily with water in the presence of a catalyst to give silanol groups and finally silica (SiO_2). Calcium and magnesium soluble sources are required to get them fully incorporated into the main matrix. Using nitrates as precursor requires its removal from the resulting material by heating it to 700 °C [28].

1.8.2 Effect of pH

The conventional sol–gel process involves an acid catalysed reaction (pH < 1) to form the silica network. This pH range may be too acidic and hinders the incorporation of a polymer into the network resulting in polymer chain scissions. Gelation process is highly dependent on the pH. It is the slowest at pH 2, which is the isoelectric point of silica. When the silica is in the anion form (SiO^{4-}) and the pH is greater than 2, hydrolysis is slow but it condenses

rapidly. Increase in pH leads to calcium incorporation without heat treatment at high temperatures [29]. The rate of silicon alkoxides hydrolysis exhibits a minimum at pH 7 and increases exponentially at both lower and higher pH values. That is in contrast with the rate of condensation, which exhibits a minimum at pH 2 and a maximum around pH 7 [30]. When pH values are high, the particulates may be highly soluble in the sol, the structure obtained was more porous. Comparatively, at low pH values network with fine pores and dense structure were obtained due to low dissolution reprecipitation rate [31].Therefore, the change in pH of the particulate silica sols is an easy tool in the design of the pore network for specific applications.

1.8.3 Temperature, aging and drying

After gel formation, next step is drying to obtain the glass/glass-ceramic. For this, drying could be performed at room temperature. Loss of water, ethanol and other volatile groups leads to shrinkage of gel. Development of high stresses may give rise to cracks. It creates additional porosity thereby distorting the structure. Addition of drying additives such as methyl or phenyl helps reduce stresses. Heating at relatively higher temperatures ranging from (40-100°C) accelerates the removal of organic species and also leads to formation of covalent Si-O-Si bonds which otherwise may not have been formed due to incomplete hydrolysis and condensation reaction. Aging at room temperature is a rather slow process and increasing the temperature may lead to increase in porosity [25].

1.8.4 Water: TEOS Molar ratio

The amount of water present in the sol-gel solution is a strong factor in determining the hydrolysis and condensation kinetics. Increase in water content with fixed TEOS concentration gives rise to increase in hydrolysis and condensation rate. Molar ratio of H_2O/Si(OR) equal to 2 is insufficient to complete the process as it leads to more open structure and less cross linking in the matrix. Water: alkoxide ratio of 4 with acid catalysed is

the ratio that is required [25]. Increase in the water content leads to a remarkable decrease in the quantity of organic species in the final product. Gelation time and pore size are also influenced by the molar ratio.

1.9 Research motivation

Calcium, magnesium, boron and fluorine are among the essential nutrients of the human body present in bones, teeth and nails. Glass/glass ceramic material is expected to deliver good bioactive properties. Melt-quenching of such a glass results in loss of fluoride during high temperature sample preparation. Sol-gel synthesis of such a composition is an interesting problem to be dealt with. However, sol-gel synthesis being a chemical route needs to be optimised.

2.0 Objectives:

I. To synthesize CaF_2-MgF_2 containing borosilicate glass-ceramics by sol-gel process.

II. To characterize as prepared glass ceramics using different spectroscopic and optical techniques such as X-ray diffraction (XRD), Fourier transform infrared spectroscopy (FTIR), Scanning electron microscopy (SEM-EDS), Thermo gravimetric analysis (TGA) and Mass plasma atomic emission spectroscopy (MP-AES).

III. To study the *in-vitro* bioactive behaviour of as prepared glass-ceramics.

References

[1] Nerem, R.M., Cellular engineering, Ann Biomed Eng, 1991, 19:529-45

[2] Langer, R., Vacanti, J.P., Tissue engineering, Science, 1993, 260: 920-26

[3] Williams, D. F., Definitions in biomaterials, Elsevier, 1987, 72

[4] Kokubo, T., Takadama, H., How useful is SBF in predicting in vivo bone bioactivity? Biomaterials, 2006, 27: 2907-15

[5] Kokubo, T., Kushitani, H., Sakka, S., Kitsugi, T., Yamamuro, T., Solutions able to reproduce in vivo surface-structure changes in bioactive glass-ceramic, J Biomed Mater Res, 1990, 24:721-34

[6] Kaur, G., Pandey, O.P., Singh, K., Homa, D., Scott, B., Pickrell, G., A review of the bioactive glasses: Their structure, properties, fabrication, and apatite formation, J. Biomed Mater Res Part A, 2014, 102A: 254-274

[7] Hench, L.L., Polak, J. M., Science, 2002, Volume 295, 5557, 1014-1017

[8] Brauer, D.S., Karpukhina, N., O'Donnell, M.D., Law, R. V., Hill, R.G., Fluoride-containing bioactive glasses: Effect of glass design and structure on degradation, pH and apatite formation in simulated body fluid, Acta Biomaterialia, 2010, 6: 3275-3282

[9] Tai, B. J., Bian, Z., Jiang, H., Greenspan, D. C., Zhong, J., Clark, A. E., Du, M. Q., Anti-gingivitis effect of a dentifrice containing bioactive glass (NovaMin) particulate, J Clin Periodontol , 2006, 33:86-91.

[10] Jones, J.R., Review of bioactive glass: From Hench to hybrids, Acta Biomaterialia, 2013, 9: 4457-4486.

[11] Gorustovich, A., Steitnetz, T., Lopez, J. P., Guglielmotti, M., Cabrini, R., Osteogenic response to bioactive glass particles modified by boron, Elsevier, 2006, 38: S1-S17

[12] Hoppe, A., Guldal, N.S., Boccaccini, A.R., A review of the biological response to ionic dissolution products from bioactive glasses and glass-ceramics, Biomaterials, 2011, 32: 2757-2774.

[13] Rude, R.K., Gruber, H.E., Norton, H.J., Wei, L.Y., Frausto, A., Kilburn, J., Dietary magnesium reduction to 25% of nutrient requirement disrupts bone and mineral metabolism in the rat bone, Elsevier, 2005, 37(2), 211-9.

[14] Rude, R.K., Gruber, H.E., Wei, L.Y., Frausto, A., Mills, B.G., Magnesium deficiency, effect on bone and mineral metabolism in the mouse. Calcif Tissue Int, 2003, 72(1), 32-41.

[15] Carlisle, E.M., Silicon: a possible factor in bone calcification, Science, 1970, 167 (3916), 279-80.

[16] Marie, P.J., The calcium-sensing receptor in bone cells: a potential therapeutic target in osteoporosis bone, Elsevier, 2010, 46(3):571-6.

[17] Karageorgiou, V., Kaplan, D., Porosity of 3D biomaterial scaffolds and osteogenesis. Biomaterials, 2005, 26(27): 5474-5491.

[18] Hench, L.L., Bioceramics, J. Am. Ceram. Soc, 1998, 81: 1705-1728.

[19] Chen, Q.Z., Thompson, I.D., Boccaccini, A.R., 45S5 Bioglass derived glass-ceramic scaffolds for bone tissue engineering, Biomaterials, 2006, 27(11): 2414-2425.

[20] Boccaccini, A.R, Chen, Q.Z., Lefebvre, L., Gremillard, L., Chevalier, J., Sintering, crystallisation and biodegradation behaviour of Bioglass derived glass–ceramics, Faraday Discuss-RSC, 2007, 136: 27-44.

[21] Kingery, W.D., Bowen, H.K., Uhlmann, D.R., Introduction to Ceramics, 2nd ed. New York: John Wiley and Sons, 1976.

[22] Fu, Q., Rahaman, M.N., Bal, B.S., Brown, R.F., Day, D.E., Mechanical and in vitro performance of 13–93 bioactive glass scaffolds prepared by a polymer foam replication technique, Acta Biomater, 2008, 4: 1854-1864.

[23] Polishchuk, S.A., Ignat'eva, L.N., Marchenko, Y.V.V.M., Oxyfluoride Glasses, 10.1134/S108765961101010X.

[24] Farooq, I., Imran, Z., Farooq, U., Leghari, A., Ali, H., Bioactive glasses: A material for future, World Journal of Dentistry, April-June, 2012, 3(2), 199-201.

[25] Milea, C.A., Bogatu, C., Duta, A., Bulletin of the Transilvania University of Brasov Series I: Engineering Sciences, 2011, Vol. 4 (53) No. 1.

[26] Hench. L.L., West, J.K., The Sol-Gel Process, Chem. Rev. 1990, 90: 33-72.

[27] Wang, D., Bierwagen, G.P., Sol-Gel Coatings on Metals for Corrosion Protection. In: Progress in Organic Coatings, Elsevier, 2009, 64: 327-338.

[28] Jones, J.R., Ehrenfried, L.M., Hench, L.L., Biomaterials, 2006, 27: 964-973.

[29] Valliant, E.M., Turdean-Ionescu, C.A., Hanna, J.V., Smith, M.E., Jones, J.R., Role of pH and temperature on silica network formation and calcium incorporation into sol–gel derived bioactive glasses J. Mater. Chem., 2012, 22, 1613.

[30] Coltrain, B.K., Melpolder, S.M., Ultrastructure Processing of Advanced Materials, New York, Wiley, 1992.

[31] Topuz, B., Ciftcioglu, M., Preparation of Particulate/Polymeric Sol-Gel Derived Microporous Silica Membranes and Determination of Their Gas Permeation Properties, J Memb Sci, 2010, 350: 42-52.

Chapter 2. Literature Review

For decades, 45S5 amorphous bioactive glass has been studied in non-load bearing applications in the biomedical industry. The literature review presented in this chapter, focuses on the synthesis of fluoride glasses/glass-ceramics. Alongside, the effect of the synthesis route on *in vitro* dissolution and mineral formation on glasses/glass-ceramics is given below:

The structural and bioactive properties of the binary glass system SiO_2-xCaO ($0<x<0.50$) were studied by Saravanapavan *et al.* [1]. The proliferation of the HCA layer is dependent on the glass composition as well as the texture of the samples. Glasses with higher concentration of calcium, larger surface area and smaller pore size have higher dissolution rate in SBF. Laczka *et al.* [2] studied the bioactive behaviour of the $54CaO\text{-}6P_2O_5\text{-}40SiO_2$, $54CaO\text{-}6P_2O_5\text{-}35SiO_2$ (mol%) systems modified using 5 mol% boron, magnesium, sodium, fluorine, and aluminium via sol-gel technique. Modifications in the gels done using aluminium were found to be amorphous, while sodium and fluoride containing gels enhanced crystallization as analysed from X-ray diffraction. The highest pore size was found for sodium modified and lowest for boron modified glass ceramics. The gel derived composition with no additives has higher pH rise from 7.4 to 9.4 whereas for melt derived glass the pH reached a maximum value of 8.0 in the simulated body fluid (SBF) solution. Effect of glass composition, dissolution medium and particle size on dissolution rate was investigated on $SiO_2\text{-}CaO\text{-}P_2O_5$ glasses with and without Na_2O by Sepulveda *et al.* [3]. With the decrease in particle size, dissolution rate increased. This gives a control over kinetics which is responsible for release of ions from the sample. The presence of proteins (from serum) in the culture medium slows down the surface reaction. SBF solution has higher dissolution rates as compared to the cell culture medium. Saravanapavan, *et al.* [4] prepared and compared the bioactivity of the gel

derived $70SiO_2$-30CaO (S70C30) composition with the melt derived quaternary composition $46.1SiO_2$-26.9CaO-$2.6P_2O_5$-$42.4Na_2O$ (45S5). The reduction in particle size of S70C30 in gel derived samples within 30 minutes of dipping in SBF confirms the ion exchange, disordering of gel network, apatite deposition which is confirmed through FTIR and N_2 sorption isotherm. The ICP analysis for Si concentration in SBF solution increased from 0.8 ppm to 55 ppm within first half an hour of dipping for gel derived sample. The results are indicative of bioactivity of S70C30 which is comparable to the 45S5 bioglass. Balas *et al.* [5] investigated the alkoxides versus nitrates precursor effect on $76SiO_2$-$23CaO$-$1P_2O_5$ (mol%) bioactive glass. Synthesis done using sol-gel technique employed inorganic salts and metal alkoxide. Comparison of results show that both the glasses exhibit bioactive behaviour *in vitro* but the glass prepared using alkoxide formed thicker and more compact apatite layer on the surface of the glasses. Uniform apatite formation leads to better site for nucleation. The biggest drawback of inorganic salts as precursors is the removal of nitrates from the final product which may lead to alteration in glass network and in turn affect its bioactivity. Balamurugam *et al.* [6] synthesized $55SiO_2$-$26CaO$-$13MgO$-$6P_2O_5$ (mol%) bioactive glass through sol-gel process and studied its chemical and textural properties. The rise in pH and the presence of Ca^{2+} and Mg^{2+} ions in simulated body fluid in the initial hours reveal the high reactivity and in turn high bioactivity of the materials. The condensation of the silanol lead to the generation of rich silica layer that crystallized to form hydroxyapatite (HAP), established through X-ray diffraction. High in-vitro bioactivity was confirmed by spheroidal morphology of HAP as observed in SEM micrograph along with the presence of Ca and P in the EDS (Energy dispersive spectroscopy). Structural properties of the borophosphate glasses with the composition $40P_2O_5$-xB_2O_3-(60- x)-Na_2O (mol %) where $10< x <25$ mol% were studied by Carta *et al.* [7]. To include B_2O_3 and P_2O_5 in the matrix, low temperature sol gel technique has been employed as the reagents used are volatile. All the organic residues were completely

eliminated from the samples at temperature <270°C. Borophosphate glasses are not entirely amorphous but in this study they prove to be bioresorbable as they do not release crystalline fragments in the dissolution medium. Brauer *et al.* [8] studied the glass series SiO_2–P_2O_5–CaO–Na_2O with increasing content of CaF_2, keeping the ratio of network former to network modifier constant. It was observed that the glass transition temperature (T_g) and crystallization onset temperature (T_c) decreased with increasing the amount of CaF_2 in the composition. The results of ^{19}F and ^{29}Si MAS NMR spectra showed that CaF_2 does not disrupts the glass network but forms mixed calcium sodium fluoride species. The synthesis of 64SiO_2–26CaO–5P_2O_5–5MgO bioactive glass was done by Saboori *et al.* [9] using the sol-gel process. The sol was kept for 10 days to allow complete hydrolysis and condensation at room temperature until gelation, followed by 3 days of heating at 70° C. Gel was further heated at 120° C to remove water completely. The synthesized bioglass revealed enhanced bioactive behaviour in SBF solution which is confirmed by apatite formation from XRD, FTIR and SEM. 700° C was choosen to be the stabilization temperature from TGA/DTA results. At higher concentrations Mg suppressed crystallization and encouraged the formation of apatite. Valliant *et al.* [10] fabricated glass monoliths with the composition 70SiO_2-30CaO mol% for different pH values from 0.5 - 5.5 and drying temperature 40°C and 600°C via sol-gel route. Samples dried at 40°C with pH >2 were found to be mesoporous. Dissolution rate of the glasses dried at 40°C was higher as compared to the ones stabilized at 600 ° C. However the porosity and strength increases with increase in stabilization temperature, along with a decrease in bioactivity. With the increase in pH from 3.2 to 5.5, pore size is observed to be increasing along with the decrease in surface area as seen from nitrogen sorption isotherm and Brunauer-Emmett-Teller (BET). Li *et al.* [11] examined the effect of partial substitution of CaO by CaF_2 on 45S5 glass, to study and compare the strength, micro hardness and bioactive behaviour. The relatively greater bond energy of Ca-F as compared to Ca-O and the

ability of CaF_2 to enhance crystallization leads to an increase in the density, micro hardness and strength of the glass. On SBF dipping, the intensity of apatite formation in CaF_2 substituted samples exhibited higher bioactivity. Ca/P ratio noted at the end of 21 days of SBF dipped samples was observed to be near to that of HAP. Jinga *et al.* [12] synthesized the system $56CaO\text{-}35.3SiO_2\text{-}7.2P_2O_5\text{-}1MgO\text{-}0.5CaF_2$ studying the bioactive behaviour with respect to calcination temperatures 700°C, 800°C, 1000°C. The increase in the calcination temperature led to increased degree of crystallinity and densification as observed from SEM. Rasberry type structure spotted in the ceramic sample calcined at 1000°C corresponding to the fluorapatite phase, while in 700 and 800°C ones a spherical morphology was observed. Delben *et al.* [13] synthesized $60SiO_2–36CaO–4P_2O_5$ (mol %) composition via sol-gel method and annealed it at 600 and 750°C, which was below the crystallization and glass transition temperature. XRD pattern of the samples showed two broad halos with no indication of crystallinity. The surface morphology as observed from SEM images revealed spheres with similar diameters ~100 nm. The Ca/P ratio of the pellets of E600 and E750 was 2.0 and 1.6 after 4 days of immersion which changed to 1.6 and 1.4 respectively after 7 days of immersion in SBF. Adams *et al*. [14] synthesized bioactive glass with the composition $50SiO_2\text{-}25Na_2O\text{-}21CaO\text{-}4P_2O_5$ (mol%) through sol-gel process using low cost sodium metasilicate, Na_2SiO_3 as silica precursor. XRD indicates the crystallization in $Na_2Ca_2Si_3O_9$ phase after 2 hours of sintering at 1000°C. Immersion of the sintered glass in SBF leads to a completely amorphous HA phase after 14 days of SBF immersion as confirmed by XRD. The materials are envisioned to be highly biocompatible and biodegradable. Abdelghany [15] explored early investigation of bioactivity in borate glasses with the compositions $70B_2O_3\text{-}15CaO\text{-}15Na_2O/LiO_2/K_2O$, and $55B_2O_3\text{-}45CaO$ (mol%). The dissolution rate of the glass samples decreases as the CaO content is increased from 15 to 45 mol%. The SEM micrograph of undipped samples show smooth surface whereas glasses immersed in sodium

phosphate medium maintained at 37°C show cottony, spherical structure which is an indication of apatite growth. Pirayesh *et al.* [16] studied the dissolution rate of sol gel synthesized glass ceramic with the composition $46.1SiO_2$-$24.4Na_2O$-$26.9CaO$-$2.6P_2O_5$ (45S5) in comparison to the melt derived composition of 45S5 bioglass. To reduce crystallization in a sample, the stabilization temperature was kept below 800° C. The fine porosity in the sol gel derived glasses acted as nucleation sites for hydroxyapatite growth. The results indicate that the heat treated gel derived samples showed slower dissolution rate but prove to be far better in terms of bioactive behaviour than amorphous glass. Chen *et al.* [17] doped CaF_2/SrF_2 into a SiO_2-P_2O_5-CaO/SrO glass system using melt quench method and investigated the *in-vitro* bioactivity of the glasses in SBF and Tris buffer solution, respectively. Results show that low fluoride content glasses were amorphous initially and dissolution took place in 3 hours from the time of immersion. Due to strong ionic strength of SBF, glass degradation and apatite formation on glass surface was slower in comparison to Tris buffer. Also it is observed that the presence of magnesium ions in the SBF solution might be the cause of hinderance and delay in the apatite process. Letaief *et al*. [18] studied the effect of aging temperature on the porosity of the glass $92SiO_2$-$6CaO$-$2P_2O_5$ (mol %) via sol-gel method. Findings of the N_2 adsorption isotherm reveal that as the number of carbon atoms increase in the surfactants $C_{10}H_{20}BrN$, $C_{19}H_{42}BrN$ and $C_{22}H_{48}BrN$, it leads to an increase in pore diameter in glasses. Formation of larger cavities is observed with the increase in synthesis temperature. BET results show that the large surface area of the glasses formed using C_{10}TAB and C_{19}TAB convert to calcium phosphate layer more rapidly. Kaur *et al.* [19] synthesized and studied the kinetics of $(25\text{-}x)CaO–\ xCuO–10P_2O_5–60SiO_2–5B_2O_3$ (where x=2.5, 5, 7.5, 10) mesoporous glasses for drug loading application. The glass with highest copper content exhibits maximum rise in pH indicating its bioactive nature. Copper enhances the exchange of ions as CuO10 glass contains apatite of particle size of 76 nm with

enhanced densification as compared to other glasses with low copper content. Samudrala *et al.* [20] synthesized calcium borosilicate glasses with the composition $31B_2O_3$-$20SiO_2$-$24.5Na_2O$-(24.5− x) CaO-x TiO_2 (mol%) (x=0, 0.5, 1, 2) via melt quench technique. The incorporation of TiO_2 leads to slow dissolution rate in physiological fluid as observed from slow pH change. As the TiO_2 content in the samples increase, the micro hardness also goes on increasing to a maximum of 576 kgf/mm^2 (Hv) for sample with highest amount of TiO_2. Chemical durability of the samples improves due to incorporation of TiO_2 in place of Si and Ca. Cytocompatibility and cell proliferation studies via MTT assay evidently reveal the nontoxic nature of the prepared glass samples.

Based on literature review one can conclude that the sol-gel techniques and related parameters play important role in the properties of samples particularly bioactivity. So, in the present study, we synthesized $52SiO_2$-$18B_2O_3$-xMgF_2-(30-x)CaF_2, (x=5,25) composition with variable process parameters. These as prepared samples are characterized and tested with different experimental techniques. The technical details and parameters used during characterization of the samples are given in the next chapter.

References

[1] Saravanapavan, P., Hench, L.L., Low-temperature synthesis, structure, and bioactivity of gel-derived glasses in the binary $CaO\text{-}SiO_2$ system, J. Biomed Mater Res, 2000, 54(4): 608-618

[2] Laczka, M., Kowalska, K.C., Osyczka, A.L., Tworzydlo, M., Turyna, B., Gel-derived materials of a $CaO\text{-}P_2O_5\text{-}SiO_2$ system modified by boron, sodium, magnesium, aluminum, and fluorine compounds, J. Biomed. Mater. Res, 2000, 52(4): 601-612

[3] Sepulveda, P., Jones, J.R., Hench, L. L., *In vitro* dissolution of melt-derived 45S5 and sol-gel derived 58S bioactive glasses, J. Biomed. Mater. Res, 2002, 61(2): 301-311

[4] Saravanapavan, P., Jones, J.R., Pryce, R.S., Hench, L.L., Bioactivity of gel– glass powders in the $CaO\text{-}SiO_2$ system: A comparison with ternary ($CaO\text{-}P_2O_5\text{-}SiO_2$) and quaternary glasses ($SiO_2\text{-}CaO\text{-}P_2O_5\text{-}Na_2O$), J. Biomed. Mater. Res Part A, 2002, 66(1): 110-119

[5] Balas, F., Regi, M.V., Ramila, A., Synthesis Routes for Bioactive Sol-Gel Glasses: Alkoxides versus Nitrates, Chem. Mater, 2002, 14: 542-548.

[6] Balamurugan, A., Balossier, G., Michel, J., Kannan, S., Benhayoune, H., Rebelo, A.H.S., Ferreira, J.M.F., Sol Gel Derived $SiO_2\text{-}CaO\text{-}MgO\text{-}P_2O_5$ Bioglass System Preparation and In Vitro Characterization, J. Biomed. Mater. Res Part B Applied Biomaterials, 2007, 83(2): 546-53

[7] Carta, D., Knowles, J.C., Guerry, P., Smith, M.E., Newport, R.J., Sol–gel synthesis and structural characterisation of $P_2O_5\text{-}B_2O_3\text{-}Na_2O$ glasses for biomedical applications, J. Mater. Chem, 2009, 19:150-158

[8] Brauer, D.S., Karpukhina, N., Law, R.V., Hill, R.G., Structure of fluoride-containing bioactive glasses, J. Mater Chem, 2009, 19: 5629-5636.

[9] Saboori, A., Rabiee, M., Moztarzadeh, F., Sheikhi, M., Tahriri, M., Karimi, M., Synthesis, characterization and in vitro bioactivity of sol-gel-derived SiO_2-CaO-P_2O_5-MgO bioglass, Mater. Sci. Eng, 2009, C 29: 335-340.

[10] Valliant, E.M., Ionescu, C.A.T., Hanna, J.V., Smith, M.E., Jones, J.R., Role of pH and temperature on silica network formation and calcium incorporation into sol–gel derived bioactive glasses, J. Mater. Chem, 2012, 22: 1613-1619.

[11] Li, H.C., Wang, D.G., Hu, J.H., Chen, C.Z., Crystallization, mechanical properties and in vitro bioactivity of sol–gel derived Na_2O-CaO-SiO_2-P_2O_5 glass-ceramics by partial substitution of CaF_2 for CaO, J. Sol-Gel Sci. Technol, 2013, 67: 56–65.

[12] Jinga, S.I., Voicu, G., Vasile, I., Badanoiun, A. I., Rev Rom Mater, 2013, 43(4): 396-401.

[13] Delben, J.R.J., Pereira, K., Oliveira, S.L., Alencar, L.D.S., Hernandes, A.C., Delben, A.A.S.T., Bioactive glass prepared by sol–gel emulsion, J. Non-Cryst. Solids, 2013, 361: 119-123.

[14] Adams, L.A., Essien, E.R., Shaibu, R.O., Oki, A., Sol-Gel Synthesis of SiO_2-CaO-Na_2O-P_2O_5 Bioactive Glass Ceramic from Sodium Metasilicate, New Journal of Glass and Ceramics, 2013, 3: 11-15.

[15] Abdelghany, A.M., Novel method for early investigation of bioactivity in different borate bio-glasses, Spectrochimica Acta Part A: Molecular and Biomolecular Spectroscopy, 2013, 100: 120-126.

[16] Pirayesh, H., Nychka, J.A., J. Am. Ceram. Soc, 2013, 96(5): 1643-1650.

[17] Chen, X., Chen, X., Brauer, D.S., Wilson, R.M., Hill, R.G,, Karpukhina, N., Bioactivity of Sodium Free Fluoride Containing Glasses and Glass-Ceramics, Materials, 2014, 7: 5470-5487.

[18] Letaief, N., Girot, A.L., Oudadesse, H., Sridi, R.D., Influence of Synthesis Parameters on the Structure, Pore Morphology and Bioactivity of a New Mesoporous Glass, J Biosci Med, 2014, 2: 57-63.

[19] Kaur, G., Pandey, O.P., Singh, K., Chudasama, B., Kumar, V., RSC Advances, 2016, 6: 51046-56.

[20] Samudrala, R., Azeem, P.A., Penugurti, V., Manavathi, B., Cytocompatibility studies of titania-doped calcium borosilicate bioactive glasses in-vitro, Mater. Sci. Eng, 2017, C 77: 772-779.

Chapter 3. Materials and methods

In this chapter, the materials and methods used for the synthesis and characterization of glass ceramic samples is given.

3.1 Chemicals used

Glass ceramics were synthesized by sol-gel method from their respective precursors in the reaction carried out in aqueous medium. All the chemicals were of analytical grade or of the highest purity available.

Table 3.1 List of chemicals used during sample preparation

Chemical name	**Chemical formula**	**Molecular weight (g/mol)**	**Company name**
Tetra Ethyl Ortho Silicate (TEOS)	$Si(OC_2H_5)_4$	208.33	ALDRICH
Boric acid	H_3BO_3	61.83	LOBA CHEMIE
Hydro fluoric acid	HF	20.01	FINE CHEM
Magnesium fluoride	MgF_2	62.30	LOBA CHEMIE
Calcium fluoride	CaF_2	78.07	SDFCL
Ethanol	C_2H_6O	46.06	MERCK
Nitric acid	HNO_3	63.01	LOBA CHEMIE
Calcium carbonate	$CaCO_3$	100.0869	LOBA CHEMIE
Magnesium Oxide	MgO	40.3044	LOBA CHEMIE

Aqueous solution of the reagents was prepared using distilled and Millipore De-Ionized Water (DI Water).

3.2 Sample preparation

The structural and bioactive properties of as prepared samples are studied with the help of X-ray diffraction (XRD), Fourier transform infrared spectroscopy (FTIR), Thermo gravimetric (TGA), Scanning electron microscope (SEM)-Energy dispersive spectroscopy (EDS) and Microwave plasma-atomic electron microscopy (MP-AES).

Glasses ceramics with the composition $52SiO_2$-$18B_2O_3$-(x) MgF_2-(30-x) CaF_2 (x =5, 25 mol %) were prepared by sol-gel route. CaF_2, MgF_2, B_2O_3, TEOS, HNO_3 with purity > 99.0% were taken as initial reagents. All the reagents were weighed on high accuracy digital weighing machine (Mettler Toledo Ml204 /A01). For preparing sample R1RT, 5ml distilled water is added to 0.3752 g $CaCO_3$ which is stirred on magnetic stirrer for 45 minutes along with drop wise addition of 0.33 ml hydrofluoric acid (HF) diluted in 5ml distilled water in a polyethylene beaker. The pH of CaF_2 is highly acidic (~2). MgF_2 is prepared by adding solution of 1.107ml HF and 3.893 ml of distilled water to 0.7557g of magnesium oxide mixed in 5ml distilled water giving the total mixture a stirring of 45 minutes. The pH of the MgF_2 solution is basic (~8-9). For 52 mol% SiO_2, 8.735ml TEOS was used as a precursor in 5ml distilled water. Stock solution of 46.777ml of distilled water with 0.433ml HNO_3 was prepared to be used as acid catalyst for silica gel synthesis. 1.6679 g of boric acid added to 3.2ml of distilled water and heated till 50°C in a glass beaker to obtain B_2O_3. Sol gel reaction was carried out in a 500 ml polyethylene beaker. Initially TEOS solution is taken in the reaction beaker, which is stirred continuously. Boric acid solution is stirred for 15 minutes and added to the stock solution is added to the TEOS solution, pH is 3. MgF_2 solution (pH=9) and CaF_2 (pH=2-3) was added drop-wise to the reaction solution after 10 minutes. After adding all the precursors, 75 ml of the reaction solution (sol) was stirred for 1hour. The pH of the solution at this point is ~8. Gelation occurred after 15 hours. It was then kept at room temperature for 3 days for aging to occur. After that the gel was dried at 100°C for 7 hours.

Sample R1-65 ($52SiO_2$-$18B_2O_3$-$25MgF_2$-$5CaF_2$) was prepared with similar procedure using distilled water. For this, the sol was kept at 65°C to form gel within 2 hours. It was kept at room temperature for the aging period of 3 days, followed by drying at 100°C for 10 hours to form powder.

Sample R2 ($52SiO_2$-$18B_2O_3$-$25MgF_2$-$5CaF_2$) was prepared in a similar manner as sample R1RT but boric acid solution was heated to ensure clear solution. Also MgF_2 solution was heated in a water bath at 60°C and ultrasonicated for 10 minutes. Gelation observed in 14 hours and it was then kept for aging for 5 days. After that the gel was divided into two halves, one half was dried in oven at 100°C for 7 hours.

Sample R3 ($52SiO_2$-$18B_2O_3$-$25MgF_2$-$5CaF_2$) was prepared with boric acid being dissolved in distilled water and heated to 55°C for 20 minutes to aid dissolution keeping the rest of the procedure to be same as sample 2. The other precursors were dissolved in de-ionized water and stirred for 30 minutes each before adding to the TEOS solution.

Sample R5 ($52SiO_2$-$18B_2O_3$-$5MgF_2$-$25CaF_2$) was prepared by dissolving boric acid powder in ethanol (35% pure) and heated till clear solution was obtained. MgF_2 and CaF_2 were used directly as powders along with 1 molar nitric acid. After gelation of the sample in glass beaker it was dried at 100°C for 24 hours. Around 3ml of the sol was kept in silica crucible (R5-CR) for direct calcination omitting the step of drying the gel.

The dried powders were initially grinded in an agate-mortar pestle. Powdered samples were used for XRD and TGA. Rest of powder is used to prepare pellets of 10 mm diameter at a pressure of 49033.25 Newton for 3 minutes. The pellets were sintered at 400°C for holding time of 2 hours in a tubular furnace. 3 pellets of each sample were prepared. One was used for XRD and FTIR characterisation. Two pellets of each sample were used to test the bioactivity in the SBF solution.

3.3 Bioactivity test

In-vitro bioactivity of the as prepared samples was checked using simulated body fluid (SBF). The solution was obtained by dissolving high purity reagents such as NaCl, $NaHCO_3$, KCl, $K_2HPO_4.3H_2O$, $MgCl.6H_2O$, 1kmol/m HCl, $CaCl_2$, Na_2SO_4, in de-ionized water. The pH of the solution was adjusted to ~7.4 using tris-hydroxymethyl aminomethane ($(CH_2OH)_3CNH_2$) and 1M HCl as demonstrated by Kokubo *et al*. [1]. The sintered pellets of each sample were dipped in SBF solution such that surface area to SBF volume ratio is $0.1cm^{-1}$[40]. Soaking of pellets in the SBF was done in polyethylene bottles for 21 and 28 days respectively. Temperature was maintained at 37°C in the incubator. The pH was recorded everyday till 21 days and 28 days. Weight of the pellets before and after immersion is recorded to find the change in weight.

3.4 Characterizations

3.4.1 X-ray diffraction (XRD)

X-rays have wavelength (λ) in the range 0.1-100Å, which is equivalent to the distances (d) between the crystal planes. The diffraction lines are obtained at particular angle of incidence (Θ), where the Bragg's law is valid i.e. $2d \sin\Theta = n\lambda$, where n is the order of diffraction. As it is an advanced technique so it gives the information about the sample up to angstrom level. It is used to determine crystallite size, phases, strain, etc.

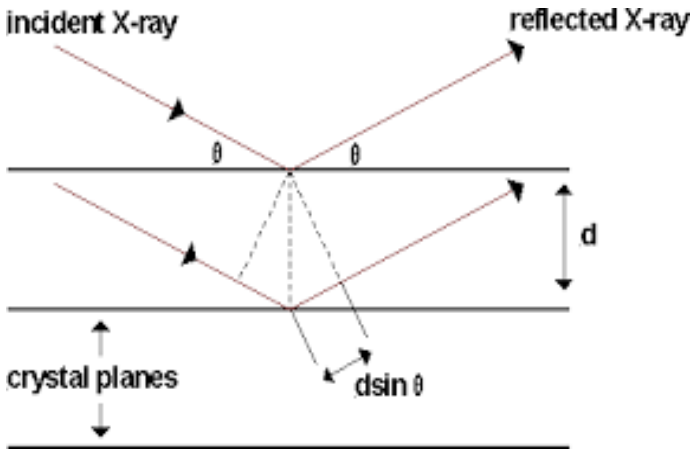

Figure 3.1 Bragg's Law in X-ray Diffraction

The XRD patterns of the synthesized and heat treated samples before SBF immersion were taken using PANalytical's X'pert Pro X-ray diffractometer using Cu K_α radiations (λ=1.54Å). The 2Θ range in which the pattern was recorded is 10-90°. XRD of the pristine and sintered samples was recorded in powder form, while the bioactivity tested pellet was taken to record the surface characteristics.

3.4.2 Fourier Transform Infrared Spectroscopy (FTIR)

This technique tells us how light interacts with matter. Sample absorbs light at each wavelength, so it is an absorption technique. It can be used to identify the bonding molecules and various functional groups. An infrared light is used, which occurs between 0.7 and 500 μm (between microwave and visible spectra). When the incoming infrared photon interacts with the molecules, absorption of the energy (which matches the frequency of vibration of the bond) takes place leading to a change in the dipole moment of the bond. After the data is collected by the detector, a mathematical algorithm is required to convert the data into spectrum. This algorithm is called Fourier transform. Every compound has its own spectrum, like a fingerprint, and this makes FTIR effective for several types of analysis. Depending on the degree of freedom of the molecule various types of vibrations like bending, stretching, rocking may take place. An FTIR spectrum of the as prepared samples was taken before and after immersion in SBF solution in the range 450-4000 cm^{-1}. It was performed to study the bioactive properties of the glass-ceramics.

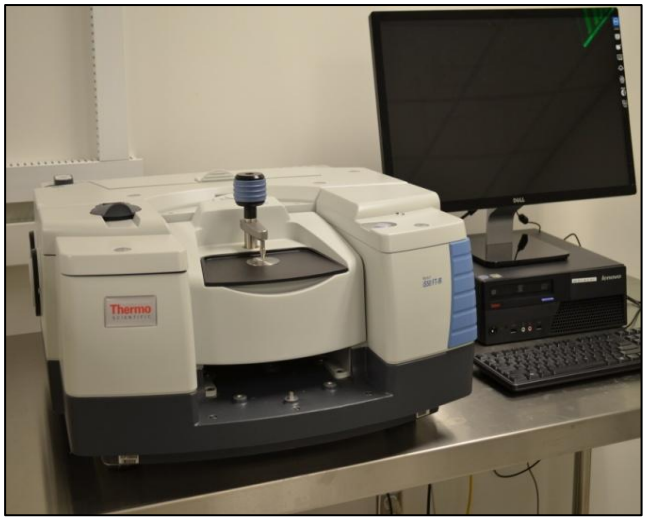

Figure 3.2 FTIR spectrometer

3.4.3 Thermo gravimetric analysis (TGA)

This technique evaluates the changes in the weight of the material as a function of time (and temperature). Calculation of the number of transformations taking place in a range of temperature along with the nature (endothermic/exothermic, physical (e.g. phase change)/chemical (e.g. decomposition)) of the transformations gives an idea of the kinetics of such transformations. The data may change depending upon heating rate, atmosphere (air, nitrogen, argon) and sample morphology (powder v/s bulk crystals), etc. The temperature of the furnace in which the sample is held is moderately increased. An analytical balance is installed outside the furnace to measure weight loss. The furnace is instructed through programme codes for either maintaining a constant heating rate, or heating to acquire a constant mass loss with time. The thermo gravimetric (TG) curve was obtained under nitrogen atmosphere that started from room temperature 30°C up to 1000 °C with the heating rate of 10 °C/min.

3.4.4 Scanning Electron Microscope (SEM) – Energy Dispersive Spectroscopy (EDS)

For surface analysis of the solid samples, SEM is a powerful technique. It is more equipped for resolving, studying the morphology with magnifying power ~ 3,000 times the optical microscope. SEM analysis is based on the interaction of electrons with the sample surface. The depth of the field is up to 100 times the optical microscope. Figure 3.3 represents the

schematic diagram for SEM. The surface morphologies and elemental compositions of the glasses were examined at room temperature using SEM-EDS at accelerating voltage 15 kV and magnification up to 1000. All the samples were gold coated for morphological study.

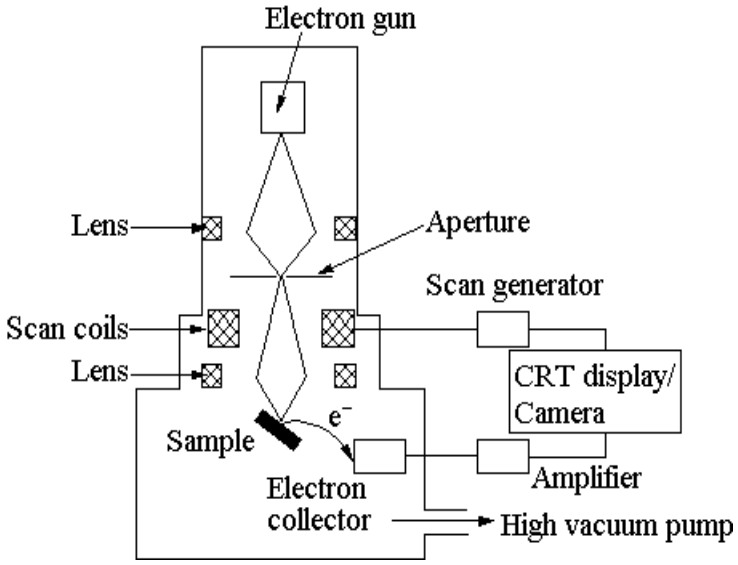

Figure 3.3 SEM microscope

Energy Dispersive Spectroscopy (EDS) enables to identify particular elements and their relative proportions in a sample. The X-ray spectrum of the sample which is bombarded by a beam of electrons is used for local analysis of chemical composition. Elements from the atomic number 4 up to 92 can be detected by the instrument.

3.4.5 Microwave plasma-atomic emission spectroscopy (MP-AES)

It is an elemental analytical technique designed to improve the scientific performance and efficiency along with being cost effective than its predecessors. The necessity for expensive gases like acetylene or nitrous oxide is eliminated as it extracts nitrogen from air to support plasma thus reducing cost and handling hassles. It uses magnetically excited nitrogen plasma that detects a range of metals and non metals. The concentration of element is observed directly from the intensity of emitted line.

Reference

[1] Kokubo, T., Kushitani, H., Sakka, S., Kitsugi, T., Yamamuro, T., Solutions able to reproduce *in vivo* surface-structure changes in bioactive glass-ceramic, J Biomed Mater Res, 1990, 24: 721-34.

Chapter 4. Results and discussions

4.1 X-ray diffraction

The X-ray diffraction patterns of the as prepared samples are shown in figure 4.1.

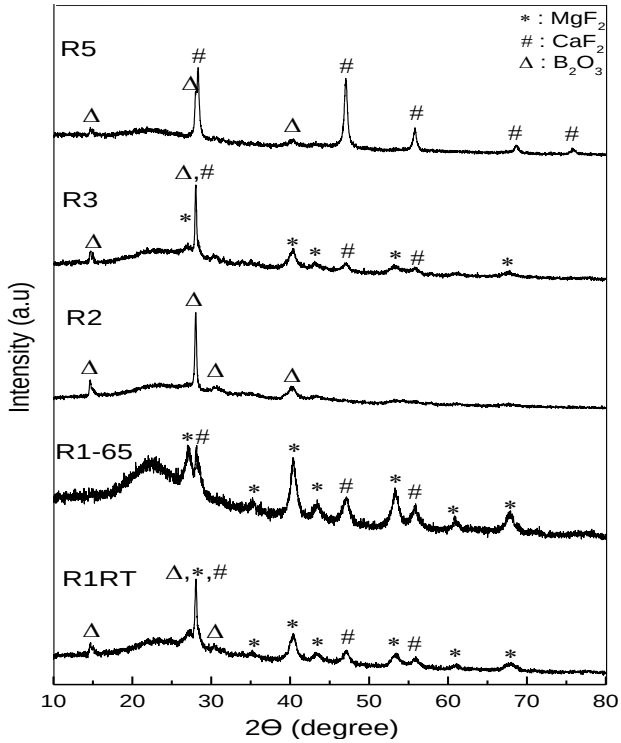

Figure 4.1 X-ray diffraction patterns of the synthesized samples.

In all the samples, broad and few peaks with broader hump are observed. Usually, the a +morphous phase is indicated by feeble broad hump at 2Θ ~20-25° which may correspond to the silicate network $(SiO_4)^-$. The peaks correspond to crystalline phases CaF_2 (ICDD No. 01-077-2094), B_2O_3 (ICDD No.00-006-0297) and MgF_2 (ICDD No. 01-072-1150). Major observed diffraction peaks are at 2θ values of 27.2, 27.7, 28.2, 40.4, 43.7, 47.0, 56.0, 67.9 degrees. Calcium and magnesium fluoride are crystallised in the glass network. Absence of borate phases in R1-65 in comparison with other samples might be because of heating of sol at 65°C to form gel. The crystalline phases CaF_2 and MgF_2 are negligibly seen in sample R2 when aging time increased from 3 days to 5 days. Due to increase in stirring and heating time for boric acid solution from 5 minutes to 20 minutes in sample R3 boric acid crystallisation intensity has reduced, as compared to R2. In R5, CaF_2 crystallizes with sharp intensity due to

presence of 25 mol% CaF_2 in this sample. It is observed that the dissolution of boric acid in distilled/de-ionized water or ethanol had negligible effect of incorporation of B_2O_3 in the sample R5.

To estimate the extent of crystallization, crystallite size and crystallinity index is calculated. Crystallite size is calculated using the Debye-Scherrer formula [1] as follows:

$$D = \frac{K\lambda}{\beta \cos\Theta} \quad (1)$$

where *D* is the crystallite size, *K* is the dimensional shape factor which 0.94 for spherical particles, λ is the source wavelength, β is the full width at half maxima (in radians), Θ is the Bragg's angle (in degrees). The crystallite size (table 4.1) lies in the range of 7-23 nm. This indicates that the crystallinity in the samples is in nanometre range. Crystallinity index (C.I) [2] is calculated using following relationship:

$$C.I = \frac{Peak\ intensity - Amorphous\ Intensity}{Peak\ intensity} \quad (2)$$

The percentage of crystalline phases like MgF_2, CaF_2 and B_2O_3 in the samples is calculated. Maximum crystallinity for MgF_2, CaF_2, B_2O_3 phases is observed in sample R1-65, R3 and R2 respectively.

The samples were heat treated up to 400°C for stabilization. After sintering, crystalline B_2O_3 phase is not visible in XRD results except in R5CR (crucible sample). The broad diffraction halo situated between 2Θ values 15° and 30° tells about vitreous nature of the sample [3,4]. In comparison to untreated sample, broadening of peaks is observed in R1RT. Significant decrease in the intensity of peaks in R2 and R3 is observed. The reason might be the absence of borate phase which leads to an increase in amorphous nature of samples. A single phase of CaF_2 (ICDD No. 01-070-1469) is detected in R5, whereas earlier there was presence of some amount of B_2O_3 phase.

Table 4.1 Crystallite size, crystallinity index of as prepared samples

	Sample Name	2Θ(degrees)	Crystallite size (nm)	Crystallinity Index
MgF_2	R1RT	40.43	8.8	0.433
	R1-65	40.39	12.2	0.501
	R2	40.39	7.1	0.277
	R3	40.39	8.7	0.374
	R5	Absent	absent	Absent
CaF_2	R1RT	47.162	12.0	0.314
	R1-65	47.088	11.8	0.322
	R2	absent	absent	absent
	R3	47.009	18.5	0.229
	R5	47.057	23.8	0.728
B_2O_3	R1RT	14.55	13.8	0.206
	R1-65	absent	absent	absent
	R2	14.55	18.0	0.358
	R3	absent	absent	absent
	R5	14.67	15.7	0.134

The use of 25 mol% calcium fluoride in R5 (direct in powder form) might have lead to the formation of calcium rich phase. R5CR was directly sintered from gel (omitting the drying step) which might have lead to incomplete embodiment of borate in amorphous structure.

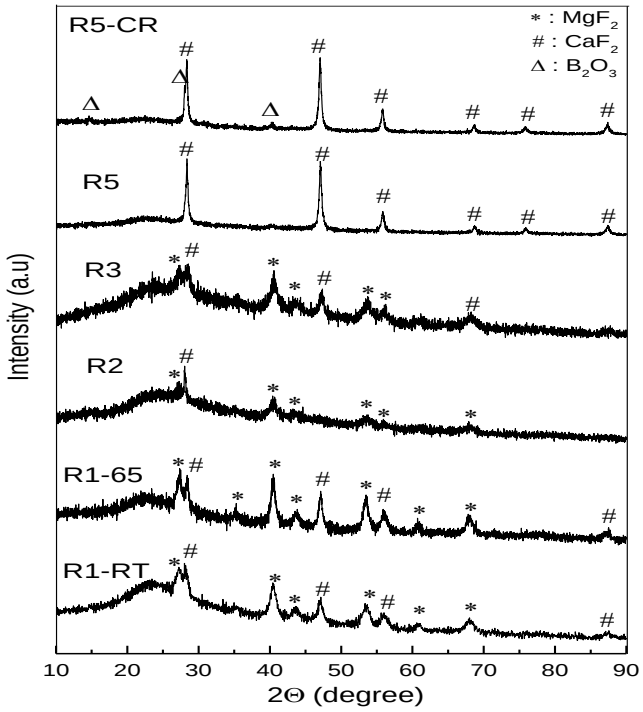

Figure 4.2 X-ray diffraction patterns of samples heat treated at 400°C for 2 hours.

Table 4.2 Crystallite size, crystallinity index of samples heat treated at 400 °C for 2 hours

	Sample Name	2Θ(degrees)	Crystallite size (nm)	Crystallinity Index
MgF_2	R1RT	40.42	8.9	0.409
	R1-65	40.47	11.9	0.523
	R2	40.66	7.4	0.249
	R3	40.50	7.9	0.341
	R5	absent	absent	absent
	R5-CR	absent	absent	absent
CaF_2	R1RT	47.03	01.0	0.325
	R1-65	47.11	17.3	0.432
	R2	47.15	12.1	0.309
	R3	47.12	18.2	0.826
	R5	47.47	23.2	0.709
	R5-CR	47.08	18.8	0.815

From table 4.2 we get the range of crystallite size to be between ~ (1.0-23) nm. In most cases, crystallinity increases after heat treatment. However in some cases, when sample is synthesized via melt-quench or sol-gel method it is observed to decrease. It may be related to diffusion of cations which leads to one metastable phase converting into another metastable phase. Because of that more strain is developed in the lattice. In the present case, it seems that the formation of in-situ phase either diffused or evaporated leads to more disordering in heat treated samples. It is also confirmed by the crystallite size which decreased after heat treatment as given in table 4.2.

4.2 Fourier Transform Infrared Spectroscopy (FTIR)

FTIR spectra of the heat treated glass-ceramic samples are shown in the figure 4.3. Major IR bands are observed at approximately 472 cm^{-1}, 807 cm^{-1}, 950 cm^{-1}, 1097 cm^{-1}, 1410 cm^{-1}, 1646 cm^{-1}, 1860 cm^{-1} in each sample with slight variations in band positions with respect to one other. The most intense and broad band can be seen from 1030-1230 cm^{-1} and 1325-1499 cm^{-1}. Peak observed at around 476 cm^{-1} corresponds to Si-O-Si bending vibration [5]. Band assigned to B-O-B stretching is at ~700 cm^{-1} [6].Vibrations in the range 850-950 cm^{-1} correspond to Si-O-2NBO vibrational mode which is linked to the presence of Ca, Mg ions in the glass network [7]. A kink for the Si-O-Si band appears at 950 cm^{-1}, which reveals that calcium in the network is forming non-bonding oxygens (NBO) [8]. Anti symmetric

stretching mode of Si-O-Si is assigned to 1110-1125 cm^{-1}[3]. Presence of boron as tetrahedral (BO^{-}_{4}) and trigonal (BO_3) units gives rise to a signal at ~950 cm^{-1} and in the range 1300-1500 cm^{-1} [9], [10]. Bend at ~2265 cm^{-1} and band in the range ~ (2500-3700) cm^{-1} corresponds to OH absorption [5]. Some amount of Ca, Mg act as modifier which can be confirmed from the presence of NBOs. XRD data (ref. section 4.1) reveal the absence of crystalline boron phases in heat treated samples. This might be associated to the diffusion of B^{3+} or BO_3 converting to BO_2 and acting as network former to promote glassy structure.

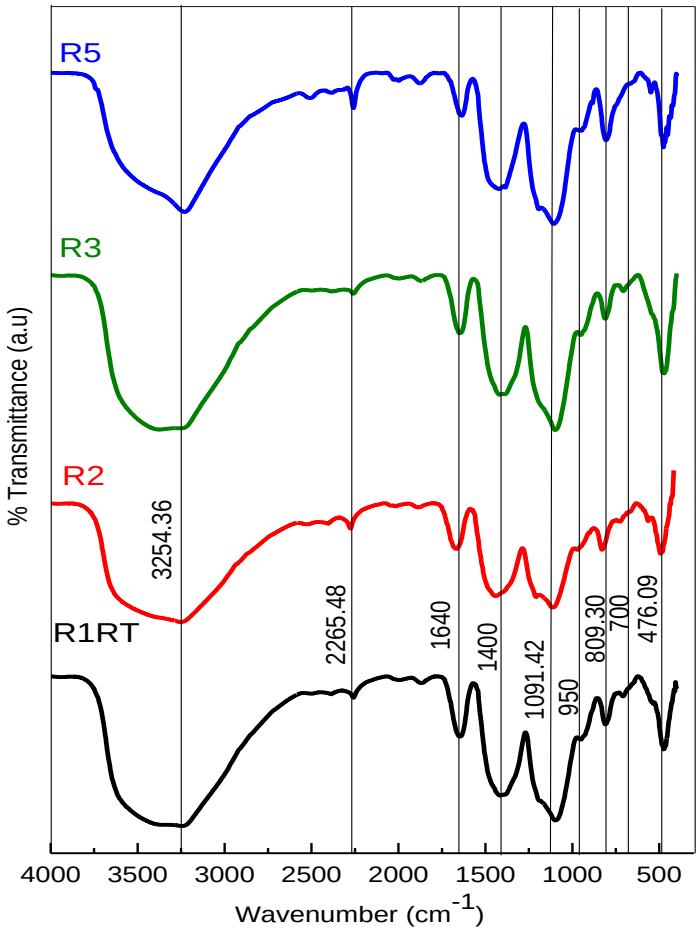

Figure 4.3 FTIR spectra of the heat treated samples at 400 °C for 2 hours

‘

Table 4.3 Peak assignment of samples heat treated at 400°C for 2 hours

Wavenumber(cm^{-1})	**Functional Group**
476.72	Rocking motion of Si-O-Si [4]
700	B-O-B [6]
809.86	Si-O-Si symmetric stretching [3]
950.16	Si-O-Si vibrational mode, stretching vibration of BO^-_4 tetrahedral units[7,10]
1091.56	Si-O-Si anti symmetric [3]
1400	B=O stretching vibration of BO_3 trigonal units [10]
1640	Bending mode of water [3]
2500-3700	OH absorption [5]

4.3 Thermo Gravimetric Analysis (TGA)

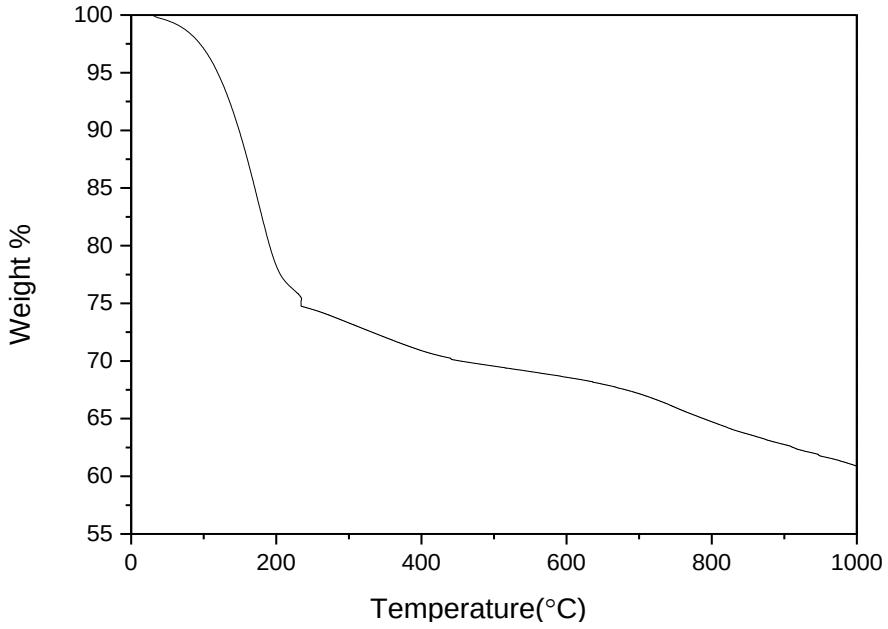

Figure 4.4 TGA plot of R3

A representation of TGA curve of sample R3 is shown in the figure 4.4. Weight loss from 30°C to 225°C is very steep due to evaporation of adsorbed water and ethanol (due to hydrolysis and polycondensation reaction [11,12]. After that the change in weight is not very drastic up to 650°C. The reagents used for sample preparation were oxides, carbonate, in addition to these nitrate group related chemicals were also present. Therefore, weight loss till high temperature (700°C) is due to the presence of nitrate group. The weight loss from 250°C to 1000°C is only 12.5% due to some organic components.

4.4 *In-vitro* bioactivity:

4.4.1 pH variation

The change in pH of the SBF solutions, in which different glass ceramic samples were dipped, was measured in order to know their dissolution behaviour. Bio glasses/ceramics usually show dissolution in SBF because of the solubility of constituent elements in the glass-ceramic. According to Hench *et al*. [13] fast exchange of modifier ions, such as Ca^{2+}, Na^{+}, takes place with H^{+} or H_3O^{+} ions from the solution. In second step, Si-O-Si bonds break such that soluble silica in the form of $Si(OH)_4$ is lost to the solution. SiO_2 rich layer is formed on the surface via condensation and repolymerization reaction as given in the following equation:

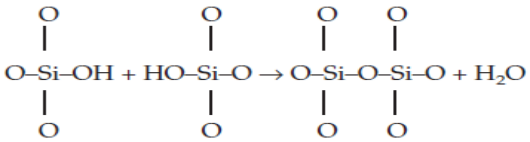

(3)

Third step leads to ionic groups such as Ca^{2+}, PO_4^{3-} migrating through SiO_2 layer to form $CaO\text{-}P_2O_5$ in turn leading to growth of an amorphous calcium phosphate takes place. Final step is the amorphous film crystallizing into HAP with the incorporation of OH^{-} or CO_3^{2-} from the SBF.

The glass-ceramic samples examined here might not have matured till last stage as proposed by Hench [13] and hence there is small variation in pH as seen from figure 4.5. As the CaF_2 content increases (in sample R5), the dissolution of the samples is not much as can be said from low pH change as compared to R1RT, R2, etc. Glass ceramics are probably more thermodynamically more stable, leading to lower release of ions such as SiO^{2+}, Ca^{2+}, etc. Glass ceramic samples reach their maximum pH within 7 days and after that the pH stayed almost constant over the remaining time of the experiment.

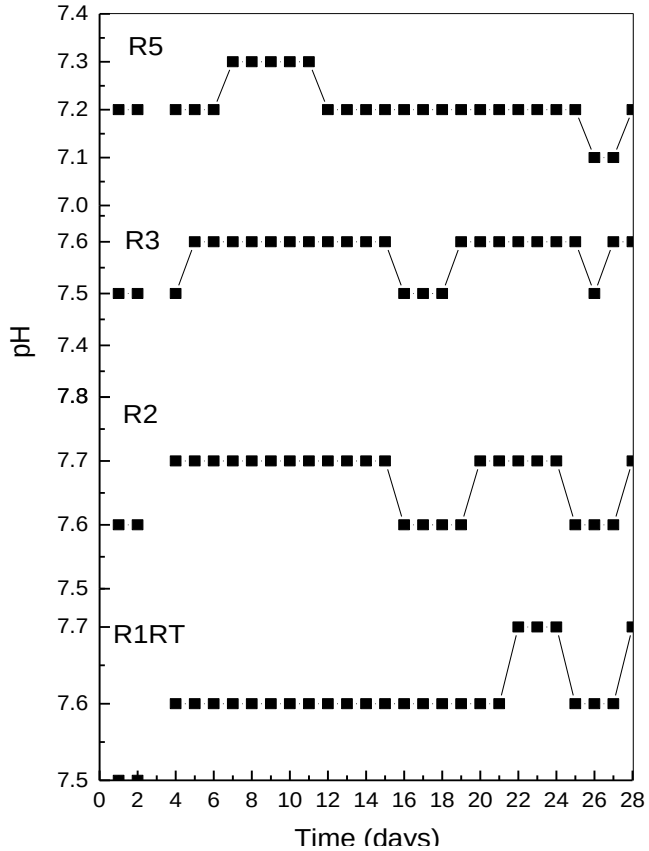

Figure 4.5 Variation of pH with time for 28 days

The above figures show the pH change with number of days. The chemical durability of the glass ceramics is higher than as observed for most glasses as low change is observed in the SBF solution [14] mainly for R5 sample with high CaF_2 content. It leads to a conclusion that samples have low dissolution rates. However, Mg^{2+} in the network favours the dissolution of

the ceramic samples leading to change in pH of R1RT as compared to R5 sample, where Ca^{2+} is in higher proportion [15].

F^- ions get exchanged for OH^- ions whereas Na^+, Ca^{2+} etc ions get exchanged for H^+. Hence for sufficient fluoride content in the glass the pH rise is less pronounced as seen from the pH table [16]. The pH <7.8 for all the dipped samples. It is probably due to pH stabilization with the increase in fluoride dissolution in SBF.

4.4.2 Weight change

Weight change (%) of the samples (20-46 % from table 4.4 and 4.5) tells about the dissolution.

Table 4.4 Weight loss as a function of 21 days immersion time.

Sample ID	**Weight of the pellets (gm)**		**Weight change (g)**	**% Weight change**
	Before immersion	**After immersion for 21 days**		
R1RTa	**0.2751**	**0.1791**	**0.096**	**34.8**
R2a	**0.063**	**0.0340**	**0.029**	**46.0**
R3a	**0.2500**	**0.1764**	**0.0736**	**29.4**
R5a	**0.2647**	**0.2093**	**0.0554**	**20.0**

Table 4.5 Weight loss as a function of 28 days immersion time.

Sample ID	**Weight of the pellets (gm)**		**Weight change (g)**	**% weight change**
	Before immersion	**After immersion for 28 days**		
R1RTb	**0.2731**	**0.2033**	**0.0698**	**25.5**
R2b	**0.1928**	**0.1220**	**0.0708**	**36.0**

R3b	**0.2613**	**0.1931**	**0.0682**	**26.0**
R5b	**0.2724**	**0.2201**	**0.0523**	**19.0**

Decrease in weight loss is due to series of rapid chemical reaction occurred when pellets of the prepared material were soaked in simulated body fluid. The reason for the change in pH of the SBF solution is due to exchange of ions from the dipped material. More dissolution leads to more weight loss, which tells about the low durability of the material and vice-versa [17]. According to literature, more the number of crystalline peaks in a sample less is the bioactivity, low is the weight change of the samples *in vitro* due to decreased dissolution (As observed in section 4.1). The same is seen from the low pH rise of the SBF solution [17, 18]. R2 has the maximum weight loss due to least crystalline structure as seen from figure 4.2. With 19%, R5-28 has minimum weight loss, this sample might be more durable (low pH change, ref. Section 4.4.1). It was observed that all samples showed nearly the same trend.

4.4.3 SEM-EDS

The SEM images for the glass ceramic samples before and after soaking in SBF are given in fig. 4.6. While fig 4.6(a) and (b) represent the micrographs of R1RT in SBF for 21 and 28 days respectively. Fig 4.6(c) and (d) represent the micrographs of R2 in SBF for 21 and 28 days. Fig 4.6e is the SEM representation of pristine R2. The SEM micrograph shows the start of visible evidence of bioactivity of the glass-ceramics. We see the formation of white precipitate on the surface of the material [10]. The morphology of the undipped sample seemed to resemble more flaky structure than dipped samples. Dipped samples seem to become porous with time due to dipping. EDS spectra of the SBF dipped samples is shown in figure 4.7. Figure 4.7(a) and (b) are for R1RT dipped in SBF for 21 and 28 days respectively. Figure 4.7(c) and (d) are for R2 dipped in SBF for 21 and 28 days respectively. Figure 4.7e is for the pristine R2. EDS was performed to assess the relative concentrations of Ca, P other

elements present on the surface as a consequence of dipping in SBF. EDS spectra reveals P was absent from pristine R2 but is present in little amounts in dipped R1RT and R2. It might have deposited from SBF solution onto the samples.

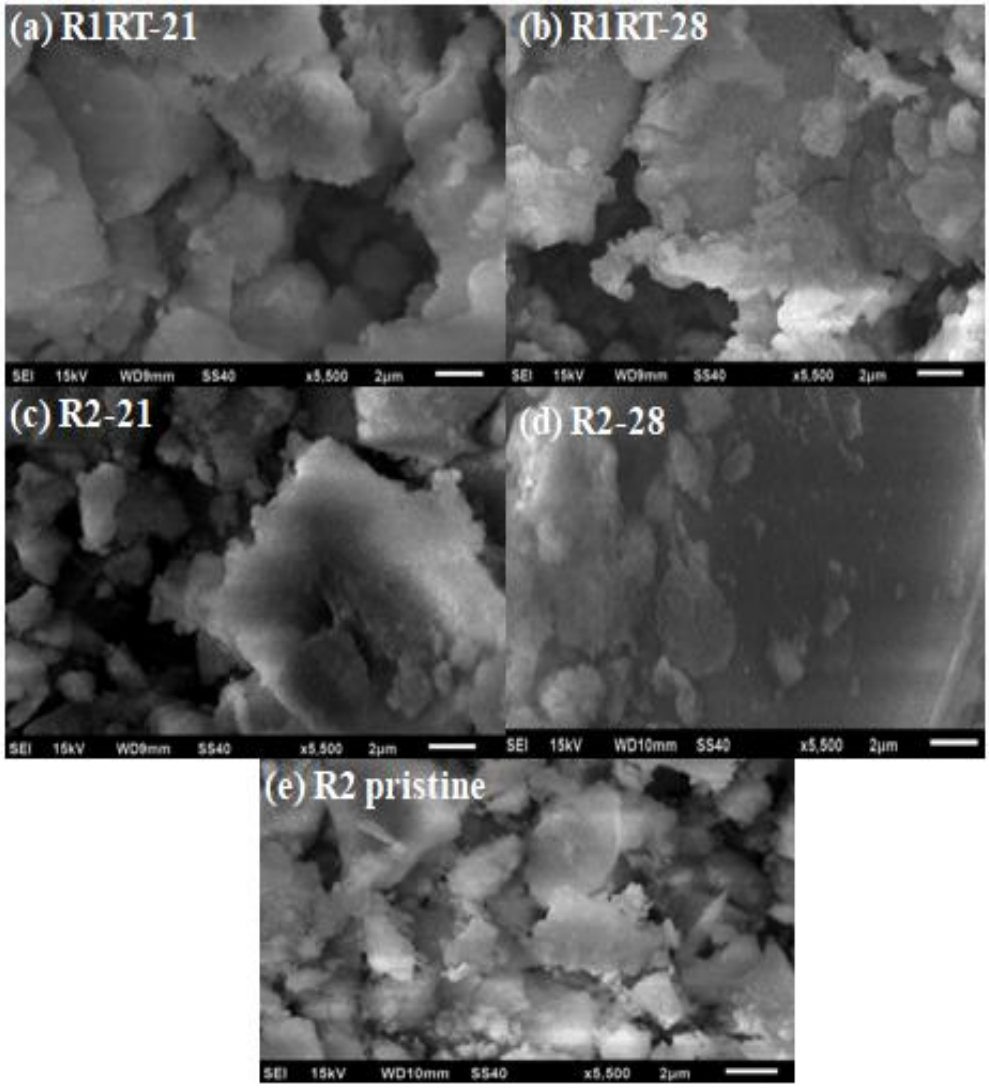

Figure 4.6 SEM images of (a) R1RT dipped 21 days (b) R1RT dipped 28 days (c) R2 dipped 21 days (d) R2 dipped 28 days (e) R2 pristine at 2µm magnification.

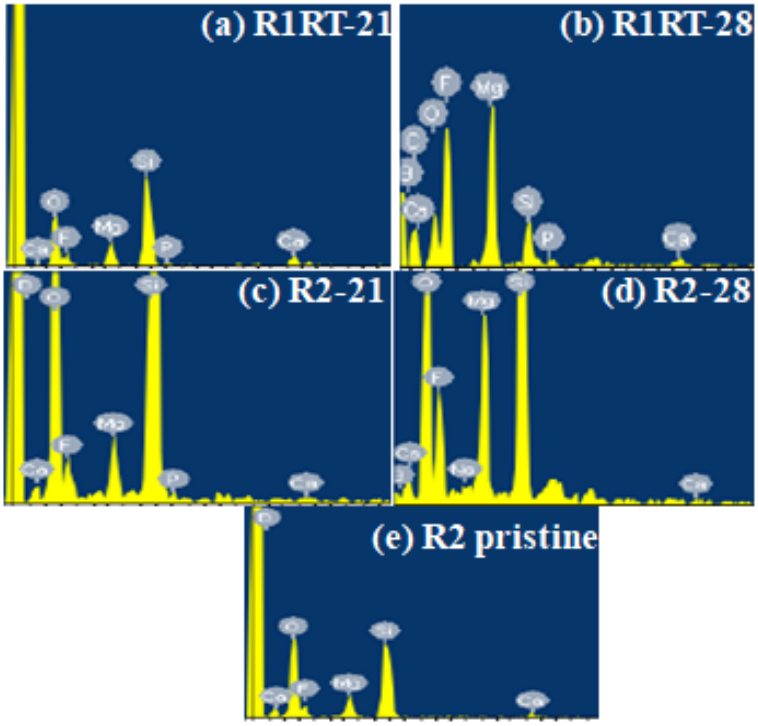

Figure 4.7 EDS spectra of (a) R1RT dipped for 21 (b) R1RT dipped for 28 days (c) R2 dipped for 21 days (d) R2 dipped for 28 days (e) R2 pristine

4.4.4 FTIR analysis of dipped samples

Compositional changes occurred in all the samples due to dipping in SBF which results in pronounced changes in the spectra in terms of changes in the band position and broadness. The band present at 476 cm^{-1} contributes for the rocking vibrations of Si–O–Si bridges [4]. Disappearance of the Si-O-Si band at 708 cm^{-1} and splitting of band at around 1400 cm^{-1} is seen. Three signals of low intensity appear at around 1365, 1480, 1505 cm^{-1}. The bands in the range ~1325-1500 cm^{-1} also indicate the HAP might be present in the samples confirming the bioactive nature of the samples [17]. Bands in figure 4.8 exhibit shift towards longer wave numbers indicating weakening of structure in comparison to undipped samples (figure 4.3). nThis might be due to structural defects triggered by the physiochemical reactions between the sample and the SBF. XRD data supports the same as shift and broadening is observed in figures 4.10 and 4.11.

Table 4.6 Peak assignment of SBF dipped samples

Wavenumber(cm^{-1})	**Group**
1325-1500	HAP [17]
3300-3700	O-H absorption [5]

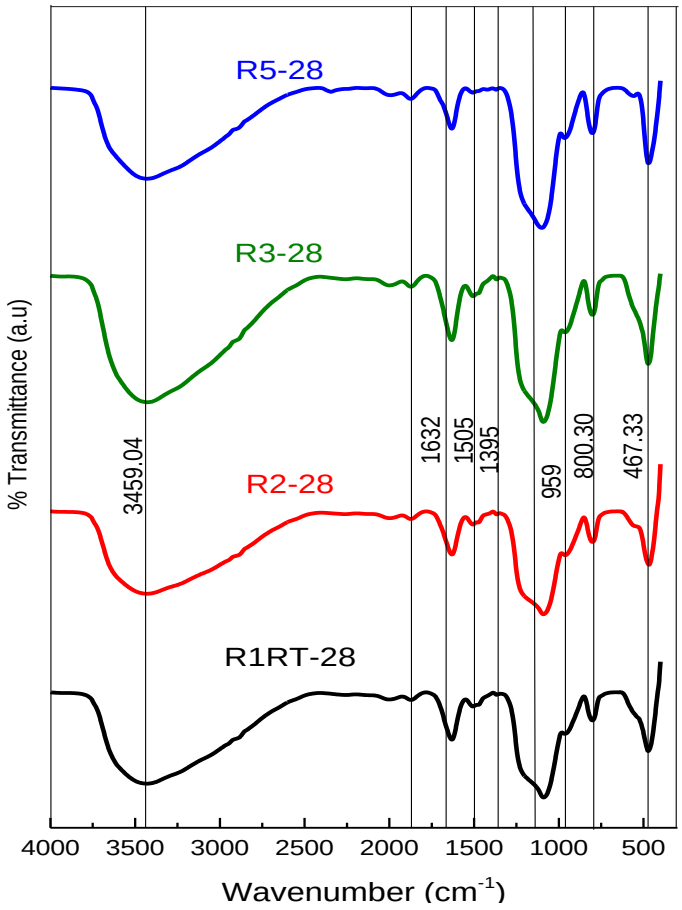

Figure 4.8 FTIR of the samples dipped in SBF solution for 28 days.

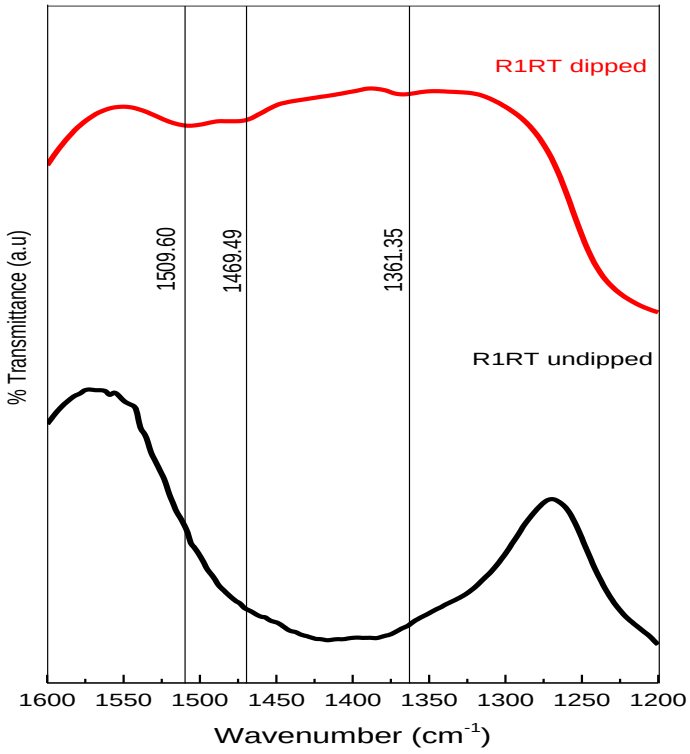

Figure 4.9 FTIR comparison of the undipped and dipped R1RT.

4.4.5 XRD (After dipping)

Figure 4.10 is the XRD plot of R1RT-heat treated (HT) and after dipping in SBF for 21 days. Figure 4.11 is the XRD plot of R2-heat treated (HT) and after dipping in SBF for 28 days. A layer of hydroxyapatite (HAP) [ICDD card no. 00-001-1008, 01-073-1731] and fluorapatite (FAP) [ICDD card no. 01-077-0120] got deposited on the samples. It means that exchange of ions between the SBF and the materials have taken place. After dipping the samples in SBF, the XRD peaks become more clear and broader as compared to heat treated samples. It seems that the amorphous part is lacking from the samples. No extra peaks are observed. Some shifting of peaks is also observed which might be due to addition of cations occupying the interstitial or proper sites. However, very clear indication in XRD, FTIR data is not observed by which the formation of FAP or HAP layer can be confirmed. XRD peaks appear to be more sharp and broadened after dipping due to amorphous part (Increase in silica concentration in MP-AES, section 4.4.6) dissolving in SBF. Along with MgF_2, which shows strong presence in partially crystallised samples, HAP and FAP phases were present.

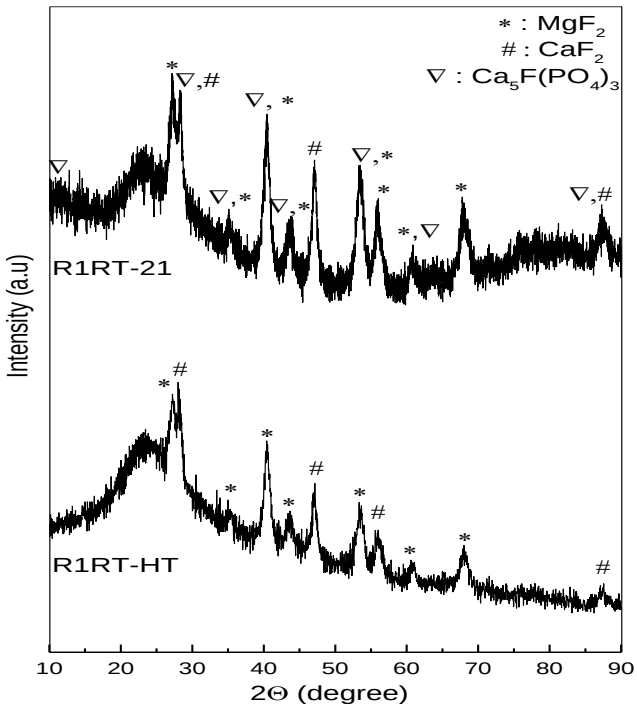

Figure 4.10 XRD of R1RT-heat treated and R1RT SBF dipped for 21 days

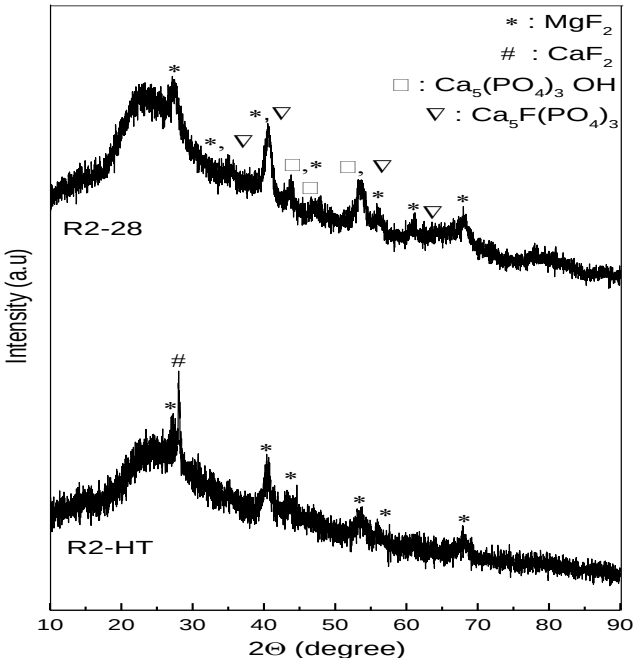

Figure 4.11 XRD of R2-heat treated and R2 SBF dipped for 28 days

4.4.6 MP-AES

MP-AES data showed the release of various ions from the sample surface into the SBF. The release of ions such as calcium, magnesium and silica ions took place from the sample surface thereby completing the first three stages of the reaction mechanism proposed by Hench [13]. It is also confirmed from the EDS analysis (section 4.4.3) that the samples are depleted of calcium which got leached out into the SBF solution. Table 4.7 shows an increase in Ca concentration. Silica release in the form of silanol groups has taken place. It plays a significant role in calcium phosphate precipitation, affecting the regeneration of the bone [19].

Table 4.7 MP-AES data for pristine SBF, R1RT- 21 days and R2-28 days

Parameter	**Pristine SBF (mg/l)**	**R1RT-21 (mg/l)**	**R2-28 (mg/l)**
Calcium	107	176	199
Magnesium	71	209	251
Silicon	<0.10	160	175

References

[1] Bindu, P., Thomas, S., Estimation of lattice strain in ZnO nanoparticles: X-ray peak profile analysis, J Theor Appl Phys, 2014, 8:123-134

[2] Segal, L., Creely, J.J., Martin, A.E., Conrad, C.M., An empirical method for estimating the degree of crystallinity of native cellulose using the X-ray diffractometer, Text. Res. J, 1959, 786-94

[3] Kaur, G., Pandey, O.P., Singh, K., Chudasama, B., Kumar, V., Combined and individual doxorubicin/vancomycin drug loading, release kinetics and apatite formation for the CaO-CuO-P_2O_5-SiO_2-B_2O_3 mesoporous glasses, RSC Adv., 2016, 6: 51046

[4] Ciceo, R.L., Trandafir, D.L., Radun, T., Ponta, O., Simon, V., Synthesis, characterisation and *in vitro* evaluation of sol–gel derived SiO_2-P_2O_5-CaO-B_2O_3 bioactive system, Ceramics International, 2014, 40: 9517–9524

[5] Adams, L.A., Essien, E.R., Shaibu, R.O., Oki, A., Sol-Gel Synthesis of SiO_2-CaO-Na_2O-P_2O_5 Bioactive Glass Ceramic from Sodium Metasilicate, New Journal of Glass and Ceramics, 2013, 3: 11-15

[6] Agathopoulos, S., Tulyaganova, D.U., Ventura, J.M.G., Kannan, S., Karakassides, M.A., Ferreira, J.M.F., Formation of hydroxyapatite onto glasses of the CaO-MgO-SiO_2 system with B_2O_3, Na_2O, CaF_2 and P_2O_5 additives, Biomaterials, 2006, 27: 1832–1840

[7] Deliormanli, A.M. Yildirim, M., Sol-gel synthesis of 13-93 bioactive glass powders containing therapeutic agents, Journal of the Australian Ceramic Society, 2016, Volume 52(2), 9-19

[8] Mukundan, L.M., Nirmal, R., Vaikkath, D. Nair, P.D., A new synthesis route to high surface area sol gel bioactive glass through alcohol washing, Biomatter, 2013, 3: 2, 24288

[9] Sorar, G.D., Dallabona, N., Gervais, C., Babonneau, F., Organically Modified SiO_2-B_2O_3 Gels Displaying a High Content of Borosiloxane Bonds, Chem Matter, 1999, 11: 910-919

[10] Samudrala, R., Reddy, G.V.N., Manavathi, B., Azeem, P.A., Synthesis, characterization and cytocompatibility of ZrO_2 doped borosilicate bioglasses, Journal of Non-Crystalline Solids, 2016, 447: 150–155

[11] Delben, J.R.J., Pereira, K., Oliveira, S.L., Alencar, L.D.S., Hernandes, A.C., Delben, A.A.S.T., Bioactive glass prepared by sol–gel emulsion, Journal of Non-Crystalline Solids, 2013, 361: 119-123

[12] Jinga, S.I., Viocu, G., Vasile, I., Badanoiu, A.I., Bioactive glass ceramic in the CaO-SiO_2-P_2O_5-CaF_2 system obtained by sol-gel method, Romanina J. of Materials, 2013, 43(4), 396-401

[13] Hench, L.L, West, J.K., Biological applications of bioactive glasses, Life Chem Reports, 1996, 13:187-241

[14] Samudrala, R., Azeem, P.A., Penugurti, V., Manavathi, B., Cytocompatibility studies of titania-doped calcium borosilicate bioactive glasses in-vitro, Materials Science and Engineering, , 2017, C 77: 772-779

[15] Saboori, A., Sheikhi, M., Moztarzadeh, F., Rabiee, M., Hesaraki, S., Tahriri, M., Sol–gel preparation, characterisation and in vitro bioactivity of Mg containing bioactive glass. Adv Appl Ceram, 2009, 108: 155-161

[16] Mneimne, M., Hill, R.G., Bushby, A.J., Brauer, D.S., High phosphate content significantly increases apatite formation of fluoride-containing bioactive Glasses, Acta Biomaterialia, 2011, 7: 1827-1834

[17] Danewalia, S.S., Singh, K., Magnetic and bioactive properties of MnO_2/Fe_2O_3 modified Na_2O-CaO-P_2O_5-SiO_2 glasses and nano crystalline glass-ceramics, Ceramics International, 2016, 42(10) : 11858-65

[18] Chen, X., Brauer, D.S., Wilson, R.M., Hill, R.G., Chen, X., Karpukhina, N., Bioactivity of Sodium Free Fluoride Containing Glasses and Glass-Ceramics, Materials, 2014, 7: 5470-5487

[19] Hench, L.L., Bioceramics, J. Am. Ceram. Soc., 1998, 81(7): 1705-28

Chapter 5 CONCLUSION AND FUTURE SCOPE

5.1 Conclusion

In the present study, process parameters are changed to synthesize borosilicate glasses with varying CaF_2 and MgF_2 concentrations. The glass is not formed in any sample. The incorporation of fluoride is possible in glasses and glass ceramics with this method which might be difficult through other method such as melt quench technique. XRD results reveal the partial crystalline nature of most of the samples. Sintering at 400°C results in broader peaks along with absence of crystalline B_2O_3 phase in all the samples. XRD and FTIR of heat treated and dipped samples show some changes which may be related to the surface modifications of glass ceramics. SEM-EDS data of dipped samples show some growth, which might be the start of HAP, FAP formation on the glass ceramic surface after 28 days of immersion. Overall, the present sample could not clearly show the formation of apatite layer.

5.2 Future scope

Longer dipping time may result in sufficient growth of FAP on the surface which is chemically more stable than HAP. Mechanical properties can be studied of the present samples to check their ability and applicability in dentistry. Moreover, the process parameters, aging time, solvents and different precursors can be tried to synthesize fluoride glasses.